

On the computation of moist-air specific thermal enthalpy.

by Pascal Marquet *Météo-France*

19th of January, 2014

Paper accepted for publication in the Quarterly Journal of the Royal Meteorological Society.

Last revised version in January 2014.

Corresponding address: pascal.marquet@meteo.fr

Abstract

The specific thermal enthalpy of a moist-air parcel is defined analytically following a method in which specific moist entropy is derived from the Third Law of thermodynamics. Specific thermal enthalpy is computed by integrating specific heat content with respect to absolute temperature and including the impacts of various latent heats (i.e., solid condensation, sublimation, melting, and evaporation). It is assumed that thermal enthalpies can be set to zero at 0 K for the solid form of the main chemically inactive components of the atmosphere (solid- α oxygen and nitrogen, hexagonal ice). The moist thermal enthalpy is compared to already existing formulations of moist static energy (MSE). It is shown that the differences between thermal enthalpy and the thermal part of MSE may be quite large. This prevents the use of MSE to evaluate the enthalpy budget of a moist atmosphere accurately, a situation that is particularly true when dry-air and cloud parcels mix because of entrainment/detrainment processes along the edges of cloud. Other differences are observed when MSE or moist-air thermal enthalpy is plotted on a psychrometric diagram or when vertical profiles of surface deficit are plotted.

1 Introduction.

This paper shows that local values of internal energy and enthalpy within a moist atmosphere can be better computed so as to study the energy and enthalpy directly for global/local domains. Difficulties encountered in the past were due to a paradox: the budget equation of temperature was easier to compute than the local values of enthalpy, whereas it was easier to compute the local values of entropy than to solve the budget equation.

One example of this paradox is given by the conservation or imbalance properties of internal energy $e_i = h - RT$ (see Appendix A) or for the enthalpy $h \equiv e_i + p/\rho$. It is important to evaluate observed changes in radiative forcing and imbalance properties for energy fluxes, in order i) to properly assess observed climate change impacts and ii) to improve our ability to understand energy changes in the climate system at regional scales. In studying the conservation of energy in NWP models and GCMs, it is common to assess global energy fluxes from the surface to the top of the atmosphere using re-analysis products. Conservation and/or imbalance properties are thus currently monitored via the computation of fluxes of energy at the surface and the top of the atmosphere rather than by directly computing regional or global integrals of energy throughout the atmosphere.

Another example of this paradox appears when the enthalpy equation is used in NWP models or in GCMs. The enthalpy equation is never written in terms of dh/dt , with the specific enthalpy h to be evaluated at each grid-point. It is recalled on the left side of Fig.(1) that the enthalpy

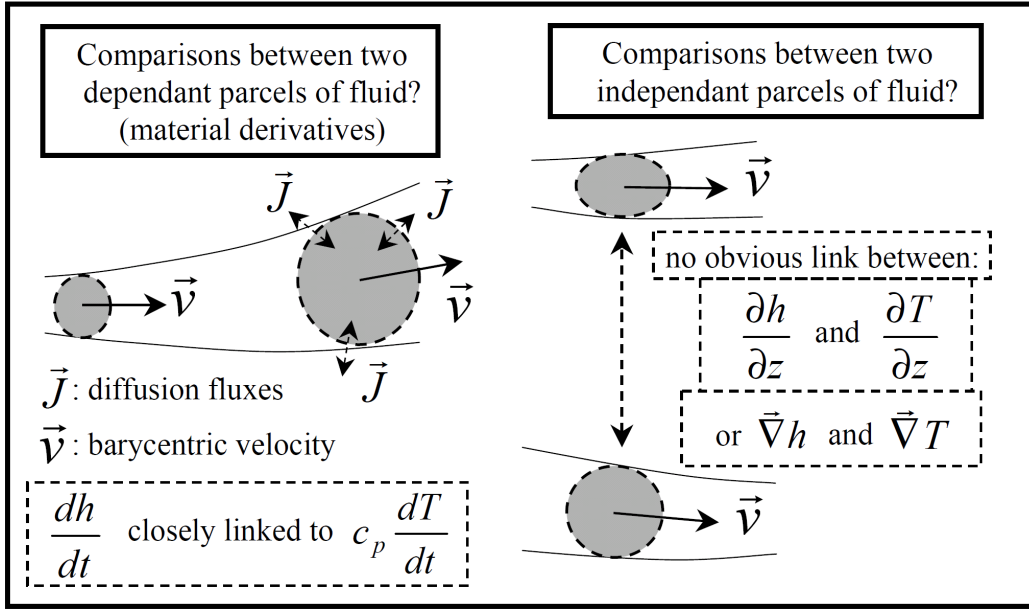


Figure 1: Comparison of enthalpy of moist-air parcels. Left panel: for parcels on a given streamline. Right panel: for parcels with different trajectories and histories.

equation can be written in terms of $c_p dT/dt$ or $d(c_p T)/dt$, where T is the temperature and c_p the moist-air specific heat. These properties are consequences of material derivatives applied to barycentric motions of open parcels of fluid described by De Groot and Mazur (1962) or Glansdorff et Prigogine (1971) and applied by Marquet (1993), Zdunkowski and Bott (2004) and Catry *et al.* (2007), among others.

It is recalled below that most of the present moist-air formulae for h and s were derived using the hypothesis of closed parcels of fluid. The problem concerning the knowledge of reference values for h or s can be briefly illustrated by starting with the dry air enthalpy written as $h_d = c_{pd} T + [(h_d)_r - c_{pd} T_r]$. This is a valid expression provided that the specific heat c_{pd} is assumed to be a constant for T close to T_r and $(h_d)_r$ is associated with T_r . The enthalpy of a clear-air parcel of moist air is computed as the sum of $q_d h_d + q_v h_v$, where h_v is computed with c_{pd} and $(h_d)_r$ replaced by c_{pv} and $(h_v)_r$. Since the term of h_d in brackets is multiplied by $q_d = 1 - q_t$, it can be neglected either if q_t is a constant or if the bracketed term is equal to zero, i.e. if $(h_d)_r = c_{pd} T_r$. But, in fact, this is not valid. It is only if q_t is a constant that changes in enthalpy or entropy can be easily computed, with no need to determine reference values for enthalpies and entropies.

The above properties are only valid if the parcels of fluid are closed. There are, however, circumstances in which it is necessary to compare absolute values of enthalpy or entropy. This is true particularly when open systems are considered and if parcels of fluid are not connected by barycentric motion. This is illustrated on the right side of Fig.(1). It is not possible to transform dh into $c_p dT$ for these independent parcels since the reference values of h and s are multiplied by varying terms, all of which depend on q_t . In consequence, spatial integrals, vertical fluxes and 3D gradients must be computed by using absolute definitions for h and s . Accordingly, Richardson (1922) and Businger (1982), hereafter referred to as R22 and B82, searched for relevant choices for zero entropy and enthalpy for both dry air and water species.

A way to compute the specific moist-air enthalpy can be found by examining the other aspect of the paradox, concerning the entropy. It is shown in the following sections that it is impossible to compute all the terms forming the entropy budget equation. Nevertheless, it is possible to use the Third Law of thermodynamics to compute the moist air entropy in an absolute way, as explained in Hauf and Höller (1987) and Marquet (2011). This is done by setting the zero of

entropies for the most stable crystalline form of all atmospheric species at 0 K.

This paper explores new possibilities for computing and analyzing isenthalpic or isentropic processes in open systems, defined by $h = \text{Constant}$ or $s = \text{Constant}$. This is equivalent to setting $dh/dt = 0$ and $ds/dt = 0$ (using barycentric formalism for the enthalpy and entropy equations). Direct local definitions for h and s may allow the study of new classes of processes associated with open systems. They include the impact of diffusion of water on h or s (entrainment and detrainment at cloud edges), and/or the impact of evaporation of water from the surface. For instance, it is reported in M11 that moist-air entropy is constant within the whole boundary layer of marine stratocumulus, with almost no jump in s at the top of the boundary layer. These properties could only be observed with the open-system formulation derived in M11, since large vertical gradients and jumps are observed for q_t , θ_l and θ_e with marine stratocumulus.

Other examples of new applications can be found in Marquet and Geleyn (2013) and Marquet (2013), where the moist-air Brunt-Väisälä frequency and potential vorticity are defined in terms of absolute values of the specific moist-air entropy derived in M11. These moist-air quantities are computed with the help of vertical and 3D gradients of s , and thus depend on relevant absolute definitions for the reference entropies of dry air and water vapour.

It is worth noting that the search for absolute and local definitions for h and s does not correspond to new definitions for the well-known potential temperatures θ'_w , θ_e or θ_l . It is shown in following sections that the absolute formulation of M11 must be understood as being a generalization to open systems of the two specific entropies derived in Pauluis *et al.* (2010, hereafter referred to as P10), which correspond to the (pseudo-) adiabatic potential temperatures θ_e or θ_l .

The important issue in this paper is to determine which kind of enthalpy might be defined in an absolute way. It is assumed that this is possible for the “thermal” enthalpies, which correspond to those enthalpies for N_2 , O_2 and H_2O substances that are generated by the variations of $c_p(T)$ generated by progressive excitations of the translational, rotational and vibrational states of the molecules, and by the possible changes of phase represented by the latent heats (with negligible impact of changes of pressure).

Both entropy and thermal enthalpy are thermodynamic state functions. Therefore, both of them can be computed following any possible reversible path that connects the dead state at 0 K and the actual atmospheric states. The Third Law of thermodynamics can be used to set the entropy to zero for the dead states corresponding to the most stable cryogenic substances at 0 K. It is assumed that the same hypothesis can be applied for thermal enthalpies at 0 K provided that the fluid is free of chemical or nuclear reactions.

The paper is organized as follows. Section 2.1 explains in some detail why the enthalpy equation can be transformed into the temperature equation, with no impact of the reference values for enthalpies. The importance of these reference values for computing the turbulent enthalpy fluxes is then illustrated in Section 2.2 using results from B82. Some impacts of reference values on the computations of moist-air entropy are described in Section 2.3, where the essential results of M11 are recalled. Comparisons between the moist-air entropy derived in M11 and those described in P10 are presented in Section 2.4. Following R22, it is explained, in Section 2.5, why it is possible to apply Nernst’s result (namely the Third Law of thermodynamics) to compute the water entropies of moist air. In Section 2.6, it is shown that the method of computing moist-air enthalpy or entropy “per unit mass of dry air” does not obviate the need to determine the reference values of moist-air species in the case of open systems. A review of different moist static energies is briefly presented in Section 2.7 in order to list these well-known quantities, which are often considered to be similar to the sum of the moist-air enthalpy and the potential energy.

Section 3 corresponds to the data and method part of the paper. The general formula for the specific moist-air thermal enthalpy is derived in Section 3.1. Computations of the standard and

reference values are then presented in Section 3.2 (details are given in Appendix B).

Numerical applications are considered in Section 4. An analysis of the validity of the approximation $(h_d)_r \approx (h_l)_r$ is shown in Section 4.1 and provides new insights into the questions raised in B82. Comparisons of the thermal enthalpy with different moist static energies are presented in Section 4.2. The properties of the moist-air thermal enthalpy diagrams are analysed in Section 4.3. Numerical values of the thermal enthalpy are computed and plotted in Section 4.4 for several stratocumulus and cumulus case studies (see Appendix C). The link between the thermal enthalpy diagram and the computation of the wet-bulb temperature are analysed in Section 4.5, where several psychrometric equations are used and compared.

In Section 5, other applications are suggested for the various findings presented in this paper.

2 Review of results of moist-air thermodynamics.

2.1 Enthalpy and temperature equations.

The enthalpy and temperature equations are described in some detail because reference will be made to them in later sections. The enthalpy equation can be written as

$$\frac{dh}{dt} = q_k \frac{dh_k}{dt} + h_k \frac{dq_k}{dt}. \quad (1)$$

Equation (1) is the development of the material derivative of the implicit weighted sum $h = q_k h_k = \sum_k q_k h_k$, where the index k applies to for dry air (d), water vapour (v), liquid water (l) and ice (i). It is assumed that it is possible to write $h_k = c_{pk} T + b_k$ for each species, where c_{pk} and b_k are constant terms attributed to each gas. Equation (2)

$$\frac{dh}{dt} = c_p \frac{dT}{dt} + h_k \frac{d_i q_k}{dt} + h_k \frac{d_e q_k}{dt} \quad (2)$$

is obtained from the properties $dh_k/dt = c_{pk} dT$ (no impact of b_k), $c_p = q_k c_{pk}$ and $dq_k/dt = d_e q_k/dt + d_i q_k/dt$. External changes $d_e q_k/dt = -\rho^{-1} \nabla \cdot J_k$ are created by the divergence of the diffusion fluxes J_k , where $J_k = \rho_k (v_k - v)$ represent departures from the barycentric mean ρv . Internal changes $d_i q_k/dt$ are created by phase changes of water.

The First Law equation (3) is expressed in terms of barycentric motion of an open parcel of fluid.

$$\frac{dh}{dt} = \frac{1}{\rho} \frac{dp}{dt} - \frac{1}{\rho} \nabla \cdot (h_k J_k) + \dot{Q}, \quad (3)$$

$$\frac{dh}{dt} = \frac{1}{\rho} \frac{dp}{dt} - \frac{1}{\rho} J_k \cdot \nabla h_k + h_k \frac{d_e q_k}{dt} + \dot{Q}. \quad (4)$$

The term involving change in pressure represents the expansion work. The divergence of the enthalpy flux $h_k J_k$ is separated into two parts in (4), with $-\rho^{-1} \nabla \cdot J_k$ equal to the external changes $d_e q_k/dt$. The heating rate \dot{Q} corresponds to other diabatic processes (mainly radiation).

The temperature equation dT/dt is then obtained by subtracting (4) from (2) and using the result $\nabla h_k = c_{pk} \cdot \nabla T$ (no impact of b_k), which leads to (5).

$$c_p \frac{dT}{dt} = \frac{1}{\rho} \frac{dp}{dt} - \frac{1}{\rho} c_{pk} J_k \cdot \nabla T - h_k \frac{d_i q_k}{dt} + Q. \quad (5)$$

The terms depending on external changes cancel out in the difference (2) minus (4). The implicit sum depending on the diffusion fluxes J_k acts in regions where gradients of temperature exist. The implicit sum depending on internal changes represents the impact of phase changes of water.

It can be written as $L_{vap} \dot{q}_{vap} + L_{sub} \dot{q}_{sub} + L_{fus} \dot{q}_{fus}$, in terms of the vaporization, sublimation and fusion rates.

Therefore all the terms in (5) can be easily computed and there is no need to determine the absolute values for enthalpies to express the First Law in terms of the temperature equation. It is also possible to compute $d(c_p T)/dt$, since it is equal to $c_p dT/dt + T dc_p/dt$ and since the sum $c_p = \sum_k q_k c_{pk}$ is known. These results correspond to the first part of the paradox.

2.2 Turbulent enthalpy fluxes: Businger (1982).

The problem of finding relevant values for the reference enthalpies $(h_k)_r$ is explicitly addressed in B82, where the specific enthalpies are written as $h_k = c_{pk} T + b_k$ (as in the previous section), corresponding to the definitions $b_k = (h_k)_r - c_{pk} T_r$ and $h_k - (h_k)_r = c_{pk} (T - T_r)$.

It is a usual practice in atmospheric science to set reference enthalpies of dry air equal to zero for a given reference temperature, typically for $T_r = 0^\circ\text{C}$. The choices of zero-enthalpy for water species are more variable. It is set to zero either for the water vapour or for the liquid water enthalpies, for the same reference temperature 0°C and with the latent heats obviously connecting the other water-enthalpies through $L_{vap} = h_v - h_l$ or $L_{fus} = h_l - h_i$. It is shown in B82 that the choices of zero-enthalpies for both dry air and liquid water are in agreement with well-established procedures for computing surface turbulent fluxes. Otherwise, additional fluxes of q_t would have to be added, leading to other definitions of the moist-air enthalpy flux. The same hypothesis $(h_d)_r = (h_l)_r = 0$ is used in the review by Fuehrer and Friehe (2002) and for $T_r = 0^\circ\text{C}$.

It is, however, unlikely that such arbitrary fluxes of q_t may be added to or subtracted from the enthalpy flux, leading to arbitrary closure for the computation of turbulent fluxes of moist air. The same is true for the vertical integral and the horizontal or vertical gradients of h , for which terms depending on q_t could be of real importance if q_t is not constant. Accordingly, one of the aims of the coming sections will be to better justify these assumptions concerning the reference values of partial enthalpies, and possibly to define them more accurately for any value of the reference temperature T_r .

Another motivation for the search for accurate definitions of moist-air enthalpy (or entropy) is to try to answer the following question illustrated on the right side of Fig.(1): Is it possible to determine whether two parcels of fluid have the same local values of h or s ?

It is easy to answer to this question for the motion of closed parcels of moist-air, for which q_t is a constant and the b_k may be cancelled, or for pseudo-adiabatic motion, for which it is possible to rely on the differential equations given by Saunders (1957) or Iribarne and Godson (1973). These differential equations are established without the need for precise definitions of partial entropies. These adiabatic or pseudo-adiabatic processes correspond to the definitions of the well-known liquid-water, equivalent and wet-bulb potential temperatures θ_l , θ_e and θ'_w , respectively.

Accordingly, the search for absolute and local definitions for h and s does not correspond to a change in the definitions of θ_l , θ_e or θ'_w and the corresponding real temperatures. A new way to answer these questions and to compute the specific moist-air “thermal enthalpy” will be found by examining the other aspect of the paradox, concerning the entropy, with the term “thermal” explained in the following sections.

2.3 Reference values of specific entropy.

The other aspect of the paradox concerns the entropy: it is easier to compute the local values of entropy than to manage its budget equation. Like the enthalpy equation (4), the entropy equation derived by De Groot and Mazur (1962) is suitable for open systems. As in Section 2.2,

the Gibbs equation (6) is expressed for barycentric motion with diffusion fluxes J_k and with the local Gibbs function defined by $\mu_k = h_k - T s_k$.

$$T \frac{ds}{dt} = \frac{dh}{dt} - \frac{1}{\rho} \frac{dp}{dt} - \mu_k \frac{dq_k}{dt}, \quad (6)$$

$$\frac{ds}{dt} = -\frac{1}{\rho} c_{pk} \frac{J_k \cdot \nabla T}{T} + s_k \frac{d_e q_k}{dt} + \frac{\dot{Q}}{T}. \quad (7)$$

The First Law expressed by (4) can be introduced in (6), leading to the entropy equation (7). A term $-(\mu_k/T) d_i q_k/dt$ should appear on the right hand side of (7) but it is equal to zero if it is assumed that changes of phases of water species are reversible and occur at equal Gibbs potential μ_k between the two phases. This excludes the possibility of supercooled water for instance.

The first reason why it is difficult to evaluate the entropy equation accurately is due to another term, \dot{S}_{irr} , which should be added into the right hand side of (7) in order to take account of other sources of irreversibility that exist in the real atmosphere. An entropy equation similar to (7) is derived in P10 for the simplified case of moist air composed of dry air, water vapour and liquid water (no ice). This equation can be rewritten as

$$\frac{ds}{dt} = \dot{S}_{irr} + \frac{\dot{Q}}{T} + (s_v - s) \dot{q}_v + (s_l - s) \dot{q}_l, \quad (8)$$

where the implicit sum $s_k d_e q_k/dt$ in (7) is expressed in (8) in terms of the rate of change of q_v and q_l due to diffusion of water vapour and precipitation processes, denoted \dot{q}_v and \dot{q}_l , respectively. The impact of the diffusion term depending on ∇T is not taken into account in (8).

Another reason why it is difficult to evaluate the entropy equations (7) or (8) accurately is due to the barycentric view, which corresponds to a unit mass of moist air. The consequence is that external input or output of q_v or q_l must be balanced at the expense of opposite changes in the moist-air value s . This explains the two terms that multiply \dot{q}_v and \dot{q}_l in (8), while s is approximated by s_d in P10.

It is thus important to determine the absolute value of s in order to compute, from (8), the impact of diffusion of water (entrainment and detrainment at the edges of clouds), or the evaporation of water from the surface. The same is true if the aim is to determine the impact of these processes on h starting from the enthalpy equation (4).

It is possible to by-pass these difficulties. The aim is to compute s directly, without trying to compute ds/dt via the associated source-sink terms. Following HH87, it is explained in M11 that it is indeed possible to compute the specific moist-air entropy by determining the reference values from the Third Law, which states that the entropy of any substance is equal to zero for the most stable crystalline form of the substance and at absolute zero temperature (the Third Law cannot be applied to liquids or gases).

A Third-Law-based formulation for the specific moist-air entropy s is written in M11 as

$$s(\theta_s) = s_{ref} + c_{pd} \ln(\theta_s), \quad (9)$$

$$\begin{aligned} \theta_s &= \theta \exp\left(-\frac{L_{vap} q_l + L_{sub} q_i}{c_{pd} T}\right) \exp(\Lambda_r q_t) \\ &\times \left(\frac{T}{T_r}\right)^{\lambda q_t} \left(\frac{p}{p_r}\right)^{-\kappa \delta q_t} \left(\frac{r_r}{r_v}\right)^{\gamma q_t} \frac{(1 + \eta r_v)^{\kappa(1 + \delta q_t)}}{(1 + \eta r_r)^{\kappa \delta q_t}}. \end{aligned} \quad (10)$$

Both s_{ref} and c_{pd} are constant terms and the entropy potential temperature θ_s depends on the adimensional parameter $\Lambda_r = [(s_v)_r - (s_d)_r] / c_{pd}$. This parameter must be evaluated from the reference values of the partial entropies of dry-air and water-vapour components.

It is important to notice that the two notions of ‘‘reference’’ and ‘‘standard’’ entropies correspond to different numerical values. The reference values $(s_v)_r$ and $(s_d)_r$ are associated with the

reference temperature T_r , the total pressure p_r , the liquid-water saturation pressure e_r and the water-vapour mixing ratio r_r . These reference values are determined according to the standard values s_v^0 and s_d^0 which correspond to the same standard values for temperature and pressure for all species, with for instance $T_0 = 0^\circ \text{C}$ (or $T_0 = 25^\circ \text{C}$) and $p_0 = 1000 \text{ hPa}$, even for water vapour. The Third-Law standard values of specific entropies are available in thermodynamic tables for all atmospheric species. The values recalled in Appendix A and computed with the datasets of Appendix B are the same as those used in HH87 and M11 (see the end of Section 3.2).

The aim of the study is thus to arrive at a formulation for the moist-air enthalpy, h , that would be similar to results (9) and (10) valid for the moist air entropy, s .

2.4 Moist entropy formulations: Pauluis *et al.* (2010).

Since the aim of the article is to compute the moist-air enthalpy by determining the reference and standard enthalpies for each species, it is important to explain why the same method is relevant for the moist-air entropy and how it is possible to recover the well-known formulae used in atmospheric science and based on the equivalent and liquid-water potential temperatures θ_e and θ_l , respectively.

A synthetic view of existing formulations of moist-air entropy derived in Iribarne and Godson, 1973, Betts, 1973 (hereafter referred to as B73); or Emanuel, 1994 (hereafter referred to as E94), is given in P10. Two moist-air entropies are defined. The first one is called ‘‘moist entropy’’ and is denoted S_m in P10. It is written as S_e in (11), since it is associated with θ_e .

$$S_e = [c_{pd} + q_t (c_l - c_{pd})] \ln \left(\frac{T}{T_r} \right) + q_v \frac{L_{vap}}{T} - q_d R_d \ln \left(\frac{p - e}{p_r - e_r} \right) - q_v R_v \ln \left(\frac{e}{e_{sw}} \right). \quad (11)$$

The second one is given by (12). It is called ‘‘dry entropy’’ and denoted S_l in P10. It is associated with the B73’ value θ_l .

$$S_l = [c_{pd} + q_t (c_{pv} - c_{pd})] \ln \left(\frac{T}{T_r} \right) - q_l \frac{L_{vap}}{T} - q_d R_d \ln \left(\frac{p - e}{p_r - e_r} \right) - q_t R_v \ln \left(\frac{e}{e_r} \right). \quad (12)$$

It is possible to show that the difference between (12) and (11) is equal to $S_e - S_l = q_t L_{vap}(T_r)/T_r$. This is slightly different from the value given in (A5) of P10 because the term e/e_{sw} was written as $e/e_{sw}(T_r)$ in (A3) of P10. The important feature is that $S_e - S_l$ depends on q_t (both here and in P10). Therefore, since there is only one physical definition for the moist-air entropy and since q_t is not a constant in the real atmosphere, S_e and S_l cannot represent the more general form of moist-air entropy at the same time.

More precisely, the comparisons between the Third Law-based formulation $s(\theta_s)$ derived in M11 and the two formulations $S_e(\theta_e)$ or $S_l(\theta_l)$ can be written as

$$s(\theta_s) = S_e(\theta_e) + q_t [(s_l)_r - (s_d)_r] + (s_d)_r, \quad (13)$$

$$s(\theta_s) = S_l(\theta_l) + q_t [(s_v)_r - (s_d)_r] + (s_d)_r. \quad (14)$$

The first result is that, if q_t is a constant, then S_e and S_l can become specialized versions of the moist-air entropy, associated with the use of the conservative variables θ_e and θ_l , respectively. However, even if S_e and S_l are equal to s up to true constant terms, the constant terms are not equal to zero and they are not the same for S_e and S_l . Moreover, they depend on the value of q_t . Therefore, even if q_t is a constant (for instance for a given vertical ascent of moist air), it is not possible to compare values of S_e or S_l with those for other columns, since the values of q_t and the ‘‘constant’’ terms in (13) and (14) differ from one column to another. This means that it is not possible to compute relevant spatial averages, fluxes or gradients of $S_e(\theta_e)$ and $S_l(\theta_l)$, because the link between θ_e or θ_l and the moist-air entropy must change in space and in time.

The other result is that, if q_t is not a constant, then $s = S_e + (s_d)_r$ only if $(s_l)_r = (s_d)_r$. Similarly, $s = S_l + (s_d)_r$ only if $(s_v)_r = (s_d)_r$. The fact that $S_e(\theta_e)$ or $S_l(\theta_l)$ may represent the moist air entropy for an open system and varying q_t is thus dependent on these arbitrary choices for the reference entropies.

Since the Third Law is a general thermodynamic property, this study considers that only the Third-Law-based formulation $s(\theta_s)$ is general enough to allow relevant computations of spatial average, fluxes or gradients of moist air entropy, and thus of θ_s . This can be taken in relation with the problem studied in B82 for computing the moist-air surface turbulent fluxes, which are performed with arbitrary choices of the reference enthalpies.

It is suggested in Appendix C of P10 that the weighted average $S_a = (1 - a)S_e + aS_l$, where a is an arbitrary constant, is a valid definition of the entropy of moist air. The adiabatic formulation S_l corresponds to $a = 1$ and θ_l , whereas the pseudo-adiabatic formulation S_e corresponds to $a = 0$ and θ_e . The weighted sum S_a applied to (13) and (14) leads to

$$s(\theta_s) = S_a + (s_d)_r + q_t \left[(s_l)_r - (s_d)_r + a \frac{L_{vap}(T_r)}{T_r} \right]. \quad (15)$$

This result (15) shows that, if the term by which q_t is multiplied is not equal to zero, S_a will be different from the Third Law formulation s . If the value $\Lambda_r \approx 5.87$ of M11 is considered, this term is equal to zero for $a = [(s_d)_r - (s_l)_r] T_r / L_{vap}(T_r) \approx 0.356$, which represents (and allows the measurement of) the specific entropy of moist air in all circumstances since no other hypothesis is made concerning the values of the reference entropies, or on adiabatic or pseudo-adiabatic properties, or on constant values for q_t . This provides another explanation for the result derived in M11: the Third-Law potential temperature θ_s is in a position about “(1 - a)” $\approx 2/3$ versus “ a ” $\approx 1/3$ between θ_l and θ_e .

The Third Law cannot be by-passed when evaluating the general formula of moist air entropy. Reference values must be set to the standard ones obtained with zero-entropy for the most stable crystalline form at $T = 0$ K. If q_t is not a constant, the formulations for $s(\theta_s)$, S_e , S_l and S_a are thus different. In M11, it is claimed that the Third-Law formulation $s(\theta_s)$ is the more general one and, in this work, we present results to further support this claim.

2.5 Richardson’s view (1922).

The issue of whether the Third Law can be applied to atmospheric studies or not, and how this can be managed practically, is an old question. Richardson (R22, pp.159-160) already wondered if it could be possible to ascribe a value to energy and entropy for a unit mass of (water) substance. He first proposed taking absolute zero temperature as the zero origin of entropies. He recognized that the entropy varied as $c_p dT/T$ and could cause the integral to take infinite values when $T = 0$ K. But he mentioned that Nernst had shown that the specific heats tended to zero at $T = 0$ K in such a way that the entropy remained finite there. This was due to Debye’s Law, which is valid for all solids and for which $c_p(T)$ is proportional to T^3 . The entropy defined by $ds = c_p dT/T$ is thus proportional to T^3 , which is not singular at $T = 0$ K.

However, Richardson did not use the Third Law and he suggested considering the lowest temperature occurring in the atmosphere (180 K) as the most practical value for the zero origin of entropies. This is in contradiction with the above conclusions of the comparisons of s , S_e and S_l , and it is shown in HH87 and M11 that it is indeed possible to use the Third Law in atmospheric science.

The Third Law is not used in P10. It is explained that the entropy of an ideal gas is fundamentally incompatible with Nernst’s theorem as it is singular for T approaching 0 K. This statement is true for ideal gases, but it does not invalidate the application of the Third Law in atmospheric

science since only the most stable solid states and Debye’s Law should be considered to apply Nernst’s theorem.

According to the advice of Richardson and to the conclusion of comparisons between the Third Law entropy with previous results recalled in S_a of P10, the aim of the article will be to mimic what is done in M11 for entropy in order to compute the thermal enthalpy (equal to the internal energy plus RT) for a unit mass of moist air.

2.6 Views “per unit mass of dry air”.

There is another possibility that could avoid the need to use absolute values for entropies or enthalpies, and thus the Third Law. The method is to assume that $q_d = 1 - q_t$ is a constant and to express moist-air entropy and enthalpy “per unit mass of dry air”, and not as specific values expressed “per unit mass of moist air”. This is the choice made, in particular, in Normand, 1921 (hereafter referred to as N21), B73 and E94, where s/q_d is expressed as any of

$$s/q_d = s_d + r_v s_v + r_l s_l, \quad (16)$$

$$s/q_d = s_d + r_t s_l + r_v (s_v - s_l), \quad (17)$$

$$s/q_d = s_d + r_t s_v - r_l (s_v - s_l), \quad (18)$$

with $r_t = r_v + r_l$ the total water mixing ratio. Similar formulae are valid for the enthalpy expressed per unit of dry air if s is replaced by h . These formulae are valid for a mixture of dry air, water vapour and liquid water, with (17) and (18) corresponding to $S_e(\theta_e)$ and $S_l(\theta_l)$ respectively.

Clearly, the term s_d can be transformed into the sum of $[s_d - (s_d)_r]$ plus $(s_d)_r$ on the right hand sides of (17) and (18). The reference value $(s_d)_r$ is a global offset having no physical meaning. The bracketed terms can be easily computed, together with $s_v - s_l$ and $s_v - s_i$ in (17) and (18), which are equal to L_{vap}/T and L_{sub}/T .

However, the reference values involved in $s_l = (s_l)_r + [s_l - (s_l)_r]$ in (17), or in $s_v = (s_v)_r + [s_v - (s_v)_r]$, in (18) are multiplied by r_t and they can be neglected if and only if r_t is a constant. Conversely, they would acquire physical meanings in the regions and for the processes where r_t is not a constant. Moreover, the study of the term s/q_d would become irrelevant for the case of open systems and varying q_d , for which it would be necessary to multiply the right hand sides by $q_d = 1 - q_t$ in order to properly compute s , with the terms $q_d (s_d)_r$ taking on a physical meaning. There is thus no real improvement with regard to the study of specific values as in (11) and (12).

The aim of the article is thus to apply the method suggested in R22 and demonstrated in M11 for the entropy, in order to derive a formulation of the specific moist-air thermal enthalpy h with a minimum of hypotheses. The result is intended to be valid for varying q_t and with the reference values of enthalpies defined from physical properties, and not prescribed arbitrarily.

2.7 A review of various MSE quantities.

Specific values of moist-air enthalpy are often computed by using the well-known MSEs. There are, however, several formulations for MSEs, each of them corresponding to different assumptions for the zero-enthalpies of dry air, water vapour or liquid-water, and to different ways of deriving MSE from either the First or Second Laws.

On the one hand, MSE formulations are derived from the Second Law and are often presented as being similar to the equivalent potential temperature θ_e , which is conserved during pseudo-adiabatic ascent or descent of moist-air parcels (N21; Madden and Robitaille, 1970; Betts, 1974; Arakawa and Schubert, 1974; E94; and Ambaum, 2010, hereafter referred to as MR70, B74, AS74 and A10).

The reason why it is possible to associate the moist-air enthalpy, h , with MSE quantities (and thus with the Second Law) is to be found in the Gibbs equation (6). If steady state vertical motions are considered, the material derivative reduces to $d/dt = w \partial/\partial z$, with all the terms in (6) being multiplied by the vertical velocity w , which can be omitted hereafter. For vertical hydrostatic motion $-\rho^{-1} \partial p/\partial z = \partial \phi/\partial z$. If the parcel is closed and undergoes reversible adiabatic processes, then $\partial s/\partial z = 0$ and $\mu_k \partial q_k/\partial z = 0$. The stationary Gibbs equation can then be written as

$$T \frac{\partial s}{\partial z} = \frac{\partial(h + \phi)}{\partial z} = 0. \quad (19)$$

The quantity $h + \phi$ is called the generalized enthalpy in A10. It is thus a quantity that is conserved for vertical motion and provided that all the previous assumptions are valid.

On the other hand, the MSEs are often interpreted as generalized forms of energy or enthalpy (First Law). For instance, the MSE function is interpreted as the non-kinetic part of the total energy in Emanuel (2004) and Peterson *et al.* (2011), with the thermal part representing the specific moist enthalpy in E94, or the fluctuating part of the total specific enthalpy of a parcel in A10.

The Third-Law-based thermal enthalpy, h , derived in the next section will be compared with a selection of existing MSE formulae, which can be written as

$$\text{MSE}_d = c_{pd} T + L_{vap} q_v + \phi, \quad (20)$$

$$\text{MSE}_l = c_{pd} T - L_{vap} q_l + \phi, \quad (21)$$

$$\text{LIMSE} = c_{pd} T - L_{vap} q_l - L_{sub} q_i + \phi, \quad (22)$$

$$h_v^* = [c_{pd} + (c_l - c_{pd}) q_t] T + L_{vap} q_v + \phi, \quad (23)$$

$$\text{MSE}_m = c_p T + L_{vap} q_v + \phi. \quad (24)$$

These MSE quantities are made up of three parts. The first part is the product of the local temperature by a moist-air specific heat, the second part is the product(s) of latent heats by specific contents, and the third part is the potential energy $\phi = g z$. The “thermal” counterparts of (20), (21), (23) and (24), where the potential energy is removed, are noted TMSE_d , TMSE_l , $h_v^* - \phi$ and TMSE_m , respectively.

The quantity MSE_d given by (20) is the most popular. It is considered in AS74 as “approximately conserved by individual air parcels during moist adiabatic processes”. Betts, 1975 (hereafter referred to as B75), mentions that it is an approximate analogue of the equivalent potential temperature θ_e . It is used as a conserved variable for defining saturated updraughts in some deep-convection schemes (Bougeault, 1985).

A liquid-water version MSE_l is defined in B75 by removing the quantity $L_{vap} q_t$ (assumed to be a constant) from (20), leading to (21). It is considered in B75 that MSE_l is an analogue of the liquid-water potential temperature θ_l . The formulation MSE_l is generalized in Khairoutdinov and Randall (2003) and in Bretherton *et al.* (2005) by removing a term $L_{sub} q_i$ from (21), for the sake of symmetry, which leads to the liquid-ice static energy given by (22). LIMSE is used as a conserved variable for defining saturated updraughts in some shallow-convection schemes (Bechtold *et al.*, 2001).

The generalized enthalpy h_v^* defined by Eq.(5.37) in A10 is given by (23). The “moist enthalpy” (per unit of dry air) defined by Eq.(4.5.4) in E94 is equivalent to $k = (h_v^* - \phi)/q_d$. Both h_v^* and k are computed in A10 and E94 with the assumptions $h_d^0 = h_l^0 = 0$. MSE is sometimes defined with c_{pd} replaced in (20) by the moist value c_p , leading to MSE_m given by (24). This version, MSE_m , is used in some convective schemes (e.g. Gerard *et al.*, 2009), because $d(c_p T)/dt$ can be easily computed from $c_p dT/dt$.

The concept of MSE was not explicitly introduced in Dufour et van Mieghem (1975, hereafter

referred to as DVM75). These authors were mainly concerned with extensive versions for enthalpy and entropy, computed for a mass m of moist air, i.e. with $H = m h$ and $S = m s$.

3 Data and method.

3.1 Specific moist-air thermal enthalpy function.

The same method already used in M11 is followed in this section to derive the formulation of the specific moist-air thermal enthalpy h in terms of a ‘‘moist enthalpy temperature’’ T_h , similar to the moist-static-energy temperature MSE_d/c_{pd} introduced in Derbyshire *et al.* (2004).

The moist atmosphere is considered as a mixture of different ideal gases, mainly composed of N_2 , O_2 , Ar and CO_2 for dry air, plus the three phases of the water species H_2O (vapour, liquid or solid). It is assumed that the volume of the condensed water species can be neglected, although their impact on the moist definitions of c_p is taken into account. The dry air is a mixture of 79 % N_2 plus 20 % O_2 , with less than 1 % of Ar, CO_2 and other gases. If the chemical reactions (like the ozone-oxygen cycle in the stratosphere) are neglected, the thermodynamic properties of dry air are thus determined at 99 % by the observed and constant concentrations of the gases N_2 and O_2 , with no tropospheric sources or sinks for these two gases.

In contrast, the specific contents for the three phases of H_2O are highly variable in time and space, with the evaporation and the precipitation processes acting as tropospheric sources and sinks, respectively. The moist atmosphere is thus a multi-component mixture of different ideal gases, i.e. dry air plus vapour, and liquid and solid water species.

Since specific enthalpy is an additive function (Dalton’s Law), the moist-air formulation is equal to the weighted average of the individual values for the partial specific enthalpies of the dry air, water vapour, liquid water and ice species, leading to

$$h = q_d h_d + q_v h_v + q_l h_l + q_i h_i. \quad (25)$$

The terms can be rearranged (with the result $q_t = q_v + q_l + q_i$), yielding

$$h = q_d h_d + q_t h_v - (q_l L_{vap} + q_i L_{sub}), \quad (26)$$

where the latent heats of vaporization and sublimation are equal to $L_{vap} = h_v - h_l$ and $L_{sub} = h_v - h_i$. As in M11, the assumption $q_d = 1 - q_t$ is made, with precipitations considered as equivalent to cloud contents and taken to be at the same temperature as the rest of the parcel. The result is

$$h = h_d + q_t (h_v - h_d) - (q_l L_{vap} + q_i L_{sub}). \quad (27)$$

The next step is to express the enthalpies by linearizing around some reference value T_r , with the hypotheses of constant values for all the specific heats c_{pd} to c_i in the atmospheric range of temperature (i.e. from 180 to 320 K). This leads to

$$h_d = (h_d)_r + c_{pd} (T - T_r), \quad (28)$$

$$h_v = (h_v)_r + c_{pv} (T - T_r), \quad (29)$$

$$h_l = (h_l)_r + c_l (T - T_r), \quad (30)$$

$$h_i = (h_i)_r + c_i (T - T_r). \quad (31)$$

The aim of the next section will be to compute the reference values $(h_d)_r$ and $(h_i)_r$, with $(h_v)_r$ and $(h_l)_r$ determined from $(h_i)_r$ by the latent heats $L_{sub}(T_r)$ and $L_{fus}(T_r)$.

If (28) and (29) are inserted into (27), and after rearrangement of the terms, the moist enthalpy can be written as

$$\begin{aligned}
h &= [(h_d)_r - c_{pd} T_r] \\
&+ c_{pd} T \left[1 + \lambda q_t - \left(\frac{L_{vap} q_l + L_{sub} q_i}{c_{pd} T} \right) \right] \\
&+ q_t [(h_v)_r - (h_d)_r - (c_{pv} - c_{pd}) T_r].
\end{aligned} \tag{32}$$

The formulation (32) is equivalently written by the system (33)-(37), in a similar way to the moist entropy formulation (9) derived in M11 in terms of θ_s , but this time in terms of a moist enthalpy temperature T_h , yielding

$$h = h_{ref} + c_{pd} T_h. \tag{33}$$

The first line of (32) defines h_{ref} by (34). The term $c_{pd} T_h$ and the dimensionless upsilon-term Υ_r correspond to the last two lines of (32), leading to (35)-(37).

$$h_{ref} = (h_d)_r - c_{pd} T_r, \tag{34}$$

$$T_h = T_{il} + \lambda T q_t + [T_r (\Upsilon_r - \lambda)] q_t, \tag{35}$$

$$T_{il} = T \left[1 - \left(\frac{L_{vap}(T) q_l + L_{sub}(T) q_i}{c_{pd} T} \right) \right], \tag{36}$$

$$\Upsilon_r = \frac{(h_v)_r - (h_d)_r}{c_{pd} T_r}. \tag{37}$$

It is worth noting that the ice-liquid temperature T_{il} corresponds to a generalization for non-zero q_i of the liquid-water (potential) temperature defined in B73 and involved in the first line of θ_s recalled in (10), in the limit where $q_i = 0$ and $\exp(-x) \approx 1 - x$ for small x . It is more general than the ice-liquid water (potential) temperature defined in Tripoli and Cotton (1981), in that the constant values $L_{vap}^0(T_0)$ and $L_{sub}^0(T_0)$ are replaced by the varying values $L_{vap}(T)$ and $L_{sub}(T)$ in (36).

In (37), the Upsilon-term Υ_r depends on the absolute values for water-vapour and dry-air enthalpies, evaluated at the temperature T_r . It acts as the dimensionless term $\Lambda_r = [(s_v)_r - (s_d)_r]/c_{pd}$ appearing in the entropy formulation (10), and it varies with T_r as illustrated in Figure 2.

It is important to demonstrate that choosing another value of T_r has no impact on h , h_{ref} and T_h as defined by (33) to (37) respectively. Otherwise, if h_{ref} could be dependent on T_r , the enthalpy temperature T_h would not be equivalent to the moist enthalpy h , as is expected, and the moist thermal enthalpy itself would not have a clear physical meaning as a state function of the moist atmosphere.

This result is true for h_{ref} because, from (34) and for constant values of c_{pd} , the variations of $(h_d)_r$ with T_r are exactly balanced by the term $-c_{pd} T_r$, leading to $(h_d)_r - c_{pd} T_r = h_d^0 - c_{pd} T_0$ which corresponds to the definition (28) applied between T_r and T_0 . The reference enthalpy (34) can thus be written as

$$h_{ref} = h_d^0 - c_{pd} T_0 \approx 256 \text{ kJ kg}^{-1}. \tag{38}$$

The numerical value 256 kJ kg^{-1} is obtained from the standard value h_d^0 determined in the next section at T_0 .

It is shown in Figure 2 that Υ_r is not a constant and decreases strongly with T_r . However, the bracketed term in (35) is a constant term independent of T_r . From the definitions $c_{pd} \lambda = c_{pv} - c_{pd}$ and (37), the term $T_r (\Upsilon_r - \lambda) q_t$ is equal to q_t times $[(h_v)_r - c_{pv} T_r] - [(h_d)_r - c_{pd} T_r]$. Moreover,

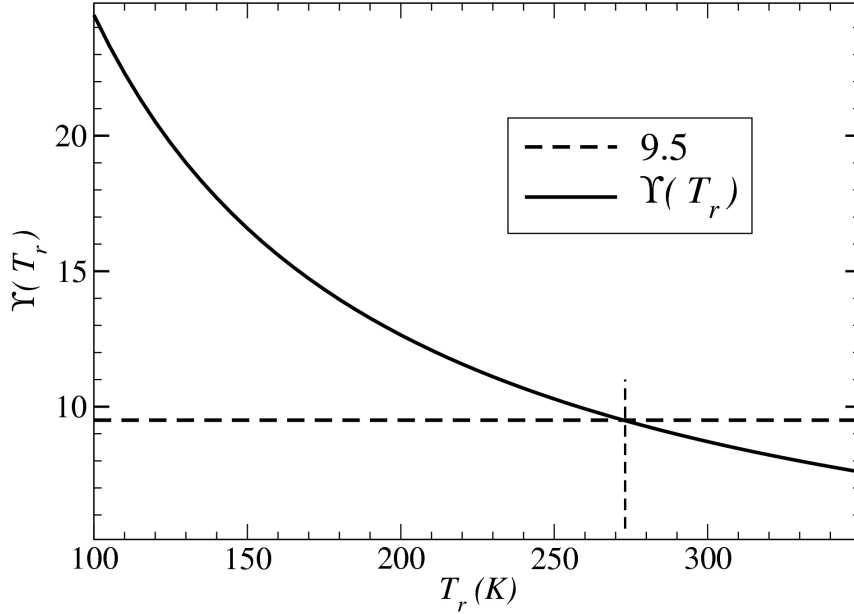


Figure 2: An analysis of the change with T_r of the upsilon term $\Upsilon_r = \Upsilon(T_r)$ (solid curve), in comparison with the constant value $\Upsilon_0 = \Upsilon(T_0) = 9.5$ (dashed straight line).

from (28) and (29), neither $(h_d)_r - c_{pd} T_r$ nor $(h_v)_r - c_{pv} T_r$ varies with T_r , as long as c_{pd} and c_{pv} are assumed to be constant terms. The result is that the bracketed term in (35) is equal to

$$T_r [\Upsilon(T_r) - \lambda] = T_0 (\Upsilon_0 - \lambda) \equiv T_\Upsilon \approx 2362 \text{ K}. \quad (39)$$

T_Υ is a constant, due to compensating variations with T_r of the two terms $T_r \Upsilon(T_r)$ and $-T_r \lambda$, as illustrated in Figure 3. The numerical value $T_\Upsilon = 2362 \text{ K}$ is obtained from the standard values given in the next section, leading to $\Upsilon_0 = \Upsilon(T_0) = (h_v^0 - h_d^0)/(c_{pd} T_0) \approx 9.5$.

An alternative, synthetic and compact expression for h defined by (33)-(39) is given by

$$\boxed{h = h_{ref} + c_{pd} T - L_{vap} q_l - L_{sub} q_i + c_{pd} (\lambda T + T_\Upsilon) q_t}. \quad (40)$$

The constant terms h_{ref} and T_Υ are given by (38) and (39).

It is worth noting that the formula (40) is symmetric with respect to the condensed water species: it is left unchanged if q_l is replaced by q_i provided that L_{vap} is replaced by L_{sub} , where L_{vap} and L_{sub} connect the water vapour with the condensed phases (q_l or q_i).

3.2 Computations of standard partial enthalpies.

One of the goals of this section is to determine the numerical values of the constants h_{ref} and T_Υ appearing in (40). They both depend, from (38) and (39), on the standard values of the partial enthalpies h_d^0 and h_v^0 . The term “standard” means that the values are expressed at the zero Celsius temperature $T_0 = 273.15 \text{ K}$ and the conventional pressure $p_0 = 1000 \text{ hPa}$. The aim of this section is thus to provide a general method for computing the partial enthalpies for several components of moist air (O_2 , N_2 , H_2O) and at any temperature, in particular for the standard conditions.

The partial enthalpies must be understood as “thermal enthalpies”, i.e. the enthalpies generated by the variations of $c_p(T)$ with T . This corresponds to progressive excitations of the translational, rotational and vibrational states of the molecules, and by the possible changes of

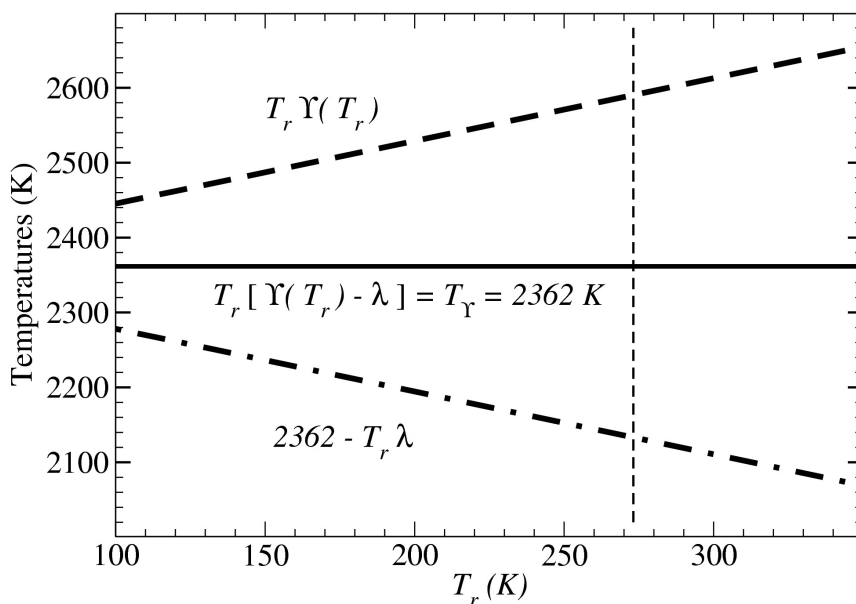


Figure 3: An analysis of the change with T_r of the three terms: “ $T_r \Upsilon(T_r)$ ” (dashed, increasing curve) ; “ $2362 - T_r \lambda$ ” (dotted-dashed, decreasing curve) and “ $T_r [\Upsilon(T_r) - \lambda]$ ” $\equiv T_\Upsilon \approx 2362$ K (solid, constant straight line).

phase represented by the latent heats (with negligible impact of changes of pressure). The consequence is that the concept of thermal enthalpy does not correspond to the concept of “standard enthalpies of formation or reaction” which are denoted by ΔH_f^0 and ΔH_r^0 and are available in chemical tables for most species.

The concepts of standard enthalpies of formation or reaction are useful in case of chemically reacting species, with the consequence that the relative concentrations of these species are determined by the equilibrium values depending on the law of mass action, depending on the reaction considered. In that case, the concentrations depend on local pressure and temperature (as in the O_3 chemistry regions). But, except in the stratosphere, the concentrations of the species are free parameters with, for instance, tropospheric water contents that are modified by diffusion, convection or precipitation processes. The standard enthalpies of formation or reaction thus cannot be relevant starting points for the determination of the tropospheric values of standard thermal enthalpies h_d^0 and h_v^0 , and thus $\Upsilon_0(T_0)$.

Moreover, in chemical thermodynamics, it is assumed that the hypothesis $\Delta H_f^0 = 0$ is valid for all gaseous forms of pure species at the conventional pressure of 1000 hPa and the standard temperature of 298 K. This is true, for instance, for O_2 and N_2 and thus for 99 % of dry air. However, since the thermal enthalpies must depend on the variations of $c_p(T)$ with T and on the latent heats, and since these quantities are different for each gas, the thermal enthalpies of O_2 and N_2 must be different in the standard conditions and $h \neq \Delta H_f^0$.

The method for computing the thermal enthalpies of N_2 , O_2 and H_2O makes use of the important result that enthalpy is a state function: it can be evaluated by following any of the reversible paths that connect the dead state at 0 K and the actual atmospheric state at temperature T .

The challenge is thus to compute the integral of $c_p(T)$ and the sum of all latent heats for a given substance from 0 K to the standard temperature T_0 , by following a reversible path involving the most stable forms of this substance at each temperature, first for the solid state(s), then for the liquid state, and finally for the gaseous form of the substance. All these processes are represented

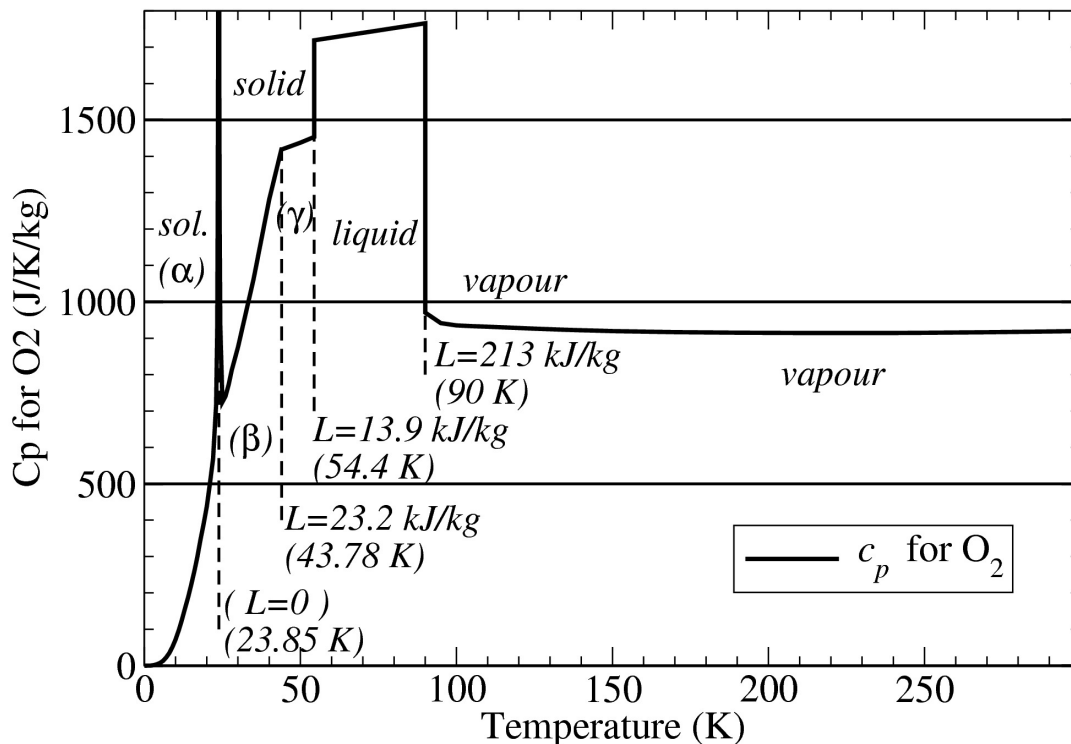


Figure 4: Specific heat capacity at constant pressure for O_2 corresponding to Table B.1 in Appendix B. Units of c_p are $J K^{-1} kg^{-1}$. The latent heats are in units of $kJ kg^{-1}$.

by the various terms of the mathematical formula

$$h^0(T_0) = h(T=0) + \int_0^{T_0} c_p(T) dT + \sum_k L_k. \quad (41)$$

Other forms of enthalpy are associated with the potential ($\phi = gz + \phi_0$), chemical or nuclear energies.

The arbitrary reference level ϕ_0 needed for defining ϕ is the same for all the molecules at a given point. The impact of ϕ_0 is thus to add or to retrieve a true constant term independent of q_v , q_l and q_i . Therefore ϕ_0 has no physical impact on the energy or on the enthalpy functions. This is true even from the barycentric standpoint of fluid dynamics, where differential fluxes of matter occur.

Nuclear reactions and the formation of atoms from elementary particles form a huge but dead state of energy in the real atmosphere. However, these forms of unavailable energy are not taken into account in this study. It is assumed that the main gases, N_2 , O_2 and H_2O , that compose the moist atmosphere only interact with the kinetic and potential energies via the standard thermal enthalpies defined by (41).

The integral of $c_p(T)$ in the thermal enthalpy formulation (41) can be computed by using the specific heats described in the Tables B.1 to B.3 for O_2 , N_2 and ice-Ih (see Appendix B). The latent heats are indicated in Figures 4, 5 and 8. The remaining problem is thus to determine the value of the thermal enthalpy at 0 K.

The standard entropies used in H87 and M11 are based on the Third Law. It is assumed that a kind of Third Law can apply to the thermal enthalpy for all substances with no chemical reaction, i.e. zero-enthalpy for $T = 0$ K.

This means that the thermal enthalpies of N_2 , O_2 and H_2O are equal to zero for the most stable solid states at 0 K (thermally dead states). Otherwise, if any indeterminacy existed for

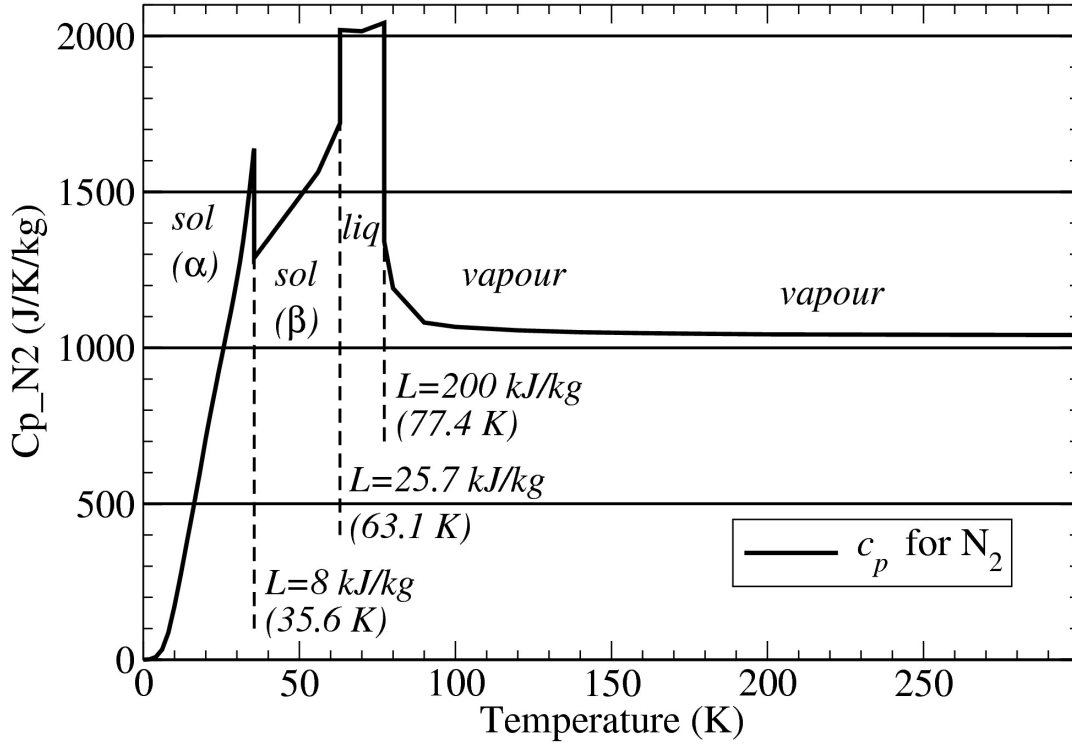


Figure 5: Specific heat capacity at constant pressure for N_2 corresponding to Table B.2 in Appendix B. Units of c_p are $J K^{-1} kg^{-1}$. The latent heats are in units of $kJ kg^{-1}$.

the values of thermal enthalpies at 0 K, except a possible identical global shift valid for all species, the thermal enthalpy of moist air could not be defined locally and would not have a clear physical meaning for all values of T_0 in (41).

The curves for the thermal enthalpies of dry-air species are shown in Figure 7. They were computed with the values of $c_p(T)$ and the latent heats given in Appendix B for O_2 and N_2 (Tables B.1 and B.2). The thermal enthalpies of O_2 and N_2 have about the same value of $477 kJ kg^{-1}$ at $T = 220 K$, with about the same value for dry air (composed at 99% of O_2 plus N_2). A thin horizontal line has been added to represent this common value $477 J kg^{-1}$.

According to Figures 4 and 5, the variation with T of specific heat for O_2 and N_2 is small above 150 K. This corresponds to constant values for c_{pd} and therefore the dry-air thermal enthalpy can be approximated by

$$h_d(T) \approx 477 kJ kg^{-1} + c_{pd} (T - 220 K) \quad (42)$$

for $T > 150 K$, leading to a standard value of h_d^0 of $530 kJ kg^{-1}$ at 273.15 K represented by the “crossed circle” symbol on Figure 7.

The curves for the thermal enthalpies of water species are depicted in Figure 8. They were computed with the values of $c_p(T)$ plotted in Figure 6 and the specific heats given in Appendix C for phase Ih of ice (Table B.3), plus the values of latent heats of fusion and vaporization L_{fus}^0 and L_{vap}^0 given in Appendix A. The latent heats of sublimation ($L_{sub} \equiv h_v - h_i$) and vaporization ($L_{vap} \equiv h_v - h_l$) are depicted by solid bold lines. The maximum at $T \approx 240 K$ for L_{sub} corresponds to a known thermodynamic property.

The same dry-air dashed line as in Figure 7 is shown in Figure 8 from 150 to 320 K, with the same “crossed circle” symbol at $T = 273.15 K$. The thin horizontal line represents the same constant value of $530 J kg^{-1}$ as plotted in Figure 7, in order to facilitate the comparison of the vertical scales in Figures 8 and 7.

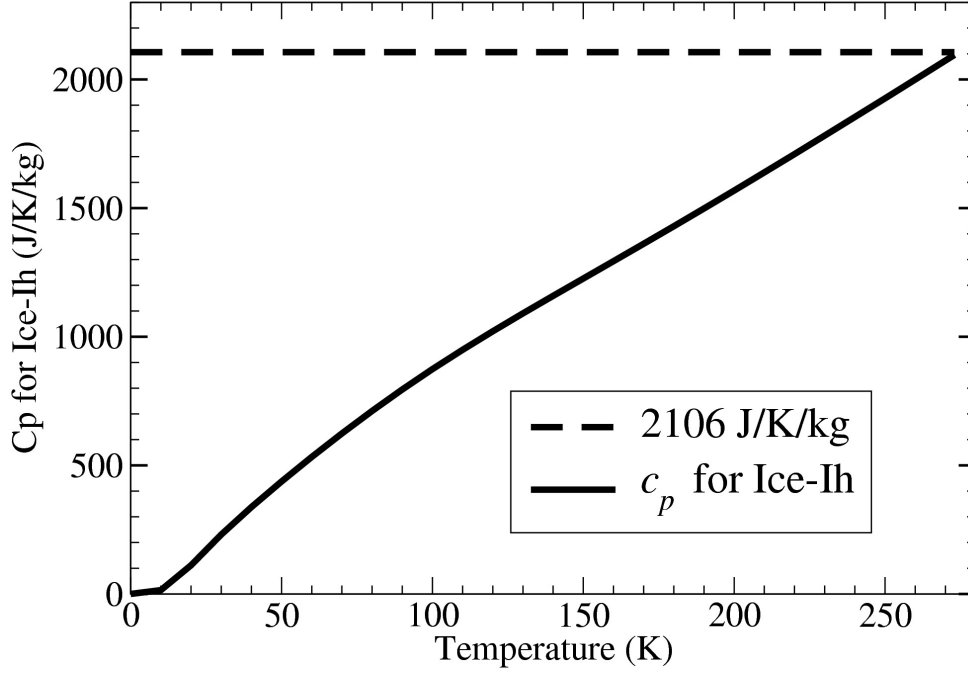


Figure 6: Specific heat capacity at constant pressure for ice-Ih (solid line) corresponding to Table B.3 in Appendix B, and the usual constant value $c_i = 2106$ (dashed line). Units are $J K^{-1} kg^{-1}$.

Finally, the values of the standard thermal enthalpies for dry-air and water species are given by

$$h_d^0 = h_d(T_0) \approx 530 \text{ kJ kg}^{-1}, \quad (43)$$

$$h_v^0 = h_v(T_0) \approx 3133 \text{ kJ kg}^{-1}, \quad (44)$$

$$h_l^0 = h_l(T_0) \approx 632 \text{ kJ kg}^{-1}, \quad (45)$$

$$h_i^0 = h_i(T_0) \approx 298 \text{ kJ kg}^{-1}. \quad (46)$$

The standard values h_d^0 and h_v^0 lead to $\Upsilon_0(T_0) \approx 9.5$ in (37), $h_{ref} \approx 256 \text{ kJ kg}^{-1}$ in (38) and $T_\Upsilon \approx 2362 \text{ K}$ in (39).

The term $T_\Upsilon/T \approx 10$ is close to $L_{vap}/(c_{pd}T) \approx 9$ and it is about ten times larger than $\lambda \approx 0.84$. This means that $c_{pd}T_\Upsilon q_t$ is a dominant term in the last term of (40), which is thus almost equal to $L_{vap} q_t$. Thus the bracketed term in (35) cannot be neglected, because it is of the same order of magnitude as the other moist terms depending on q_t , q_l or q_i in (36).

If the specific heat for dry air, ice, liquid water and water vapour are assumed to be constant with T above 150 K, the thermal enthalpies can be approximated by

$$h_d(T) \approx h_d^0 + c_{pd}(T - T_0), \quad (47)$$

$$h_v(T) \approx h_v^0 + c_{pv}(T - T_0), \quad (48)$$

$$h_l(T) \approx h_l^0 + c_l(T - T_0), \quad (49)$$

$$h_i(T) \approx h_i^0 + c_i(T - T_0). \quad (50)$$

Reference values are computed with $T = T_r$ in (47)-(50).

The important result is that hypotheses of linear laws ($h_k \approx c_{pk}T$) for enthalpies of dry-air or water species are clearly invalidated since the straight lines $h_k(T)$ intersect at 0 K in Figure 8, at the non-zero values $h_k^0 - c_{pk}T_0$.

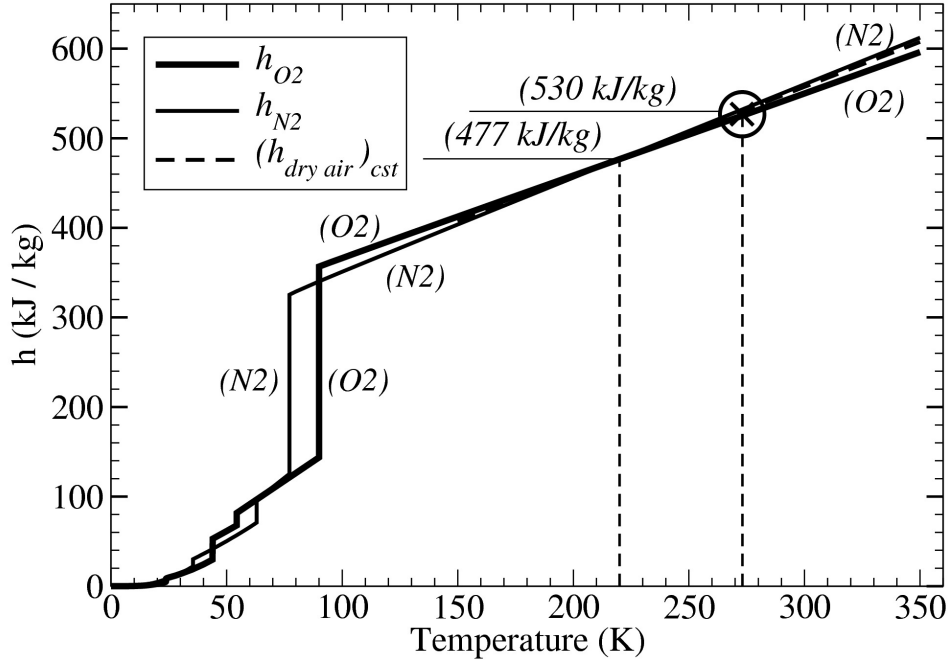


Figure 7: Enthalpies for O_2 (bold solid line) and N_2 (thin solid line) as a function of the absolute temperature, with units of kJ kg^{-1} . The dry-air curve (dashed line) represents the dry-air enthalpy (h_d), computed and plotted from 100 to 320 K with the “constant specific heat capacity” assumption ($c_{pd} = 1004.7 \text{ J K}^{-1} \text{ kg}^{-1}$).

It is worth noting that the same dataset used to compute the standard values of enthalpies can be used to compute the standard values of entropies for O_2 , N_2 and H_2O . It is important to check this so as to demonstrate the good level of accuracy of the dataset and method described in this section. The results (not shown) indicated that the standard entropies are close to the values published in HH87 and used in M11: 0.5% deviation for N_2 vapour, 1.3% for O_2 vapour and 0.2% for ice, including a residual entropy of $189 \text{ J K}^{-1} \text{ kg}^{-1}$ for ice-Ih at 0 K due to proton disorder and to the remaining randomness of hydrogen bonds at 0 K (Pauling, 1935, Nagle, 1966).

4 Results.

4.1 Impacts of a coincidence and of Trouton’s rule.

It is assumed in many studies (B82, E94 or A10) that $h_d(T_0) \approx h_l(T_0)$ at $T_0 = 0^\circ \text{ C}$ and that this common value for the enthalpies is equal to zero. The accuracies of these two approximations are analyzed in this section.

The special temperature for which $h_d(T) = h_l(T)$ can be computed by setting (47) and (49) equal. The result $241.4 \text{ K} = -31.75^\circ \text{ C}$ is precisely the temperature for which the curves for dry-air and liquid-water enthalpies intersect in Figure 8. However, the difference $h_d(T) - h_l(T)$ is positive and becomes progressively larger for increasing temperatures and in particular for temperatures that are positive on the Celsius scale.

The first hypothesis $h_d(T_0) \approx h_l(T_0)$ is thus an approximation based on a coincidence. It is not a fundamental physical property and it is not valid for all temperatures. This means that it could be worthwhile to avoid this approximation and to compute the moist-air enthalpy by (40) and with the more accurate observed values for $h_d(T)$ and $h_l(T)$ given by (47) and (49).

The second hypothesis is that both $h_d(T_0)$ and $h_l(T_0)$ could be equal to zero, or that they

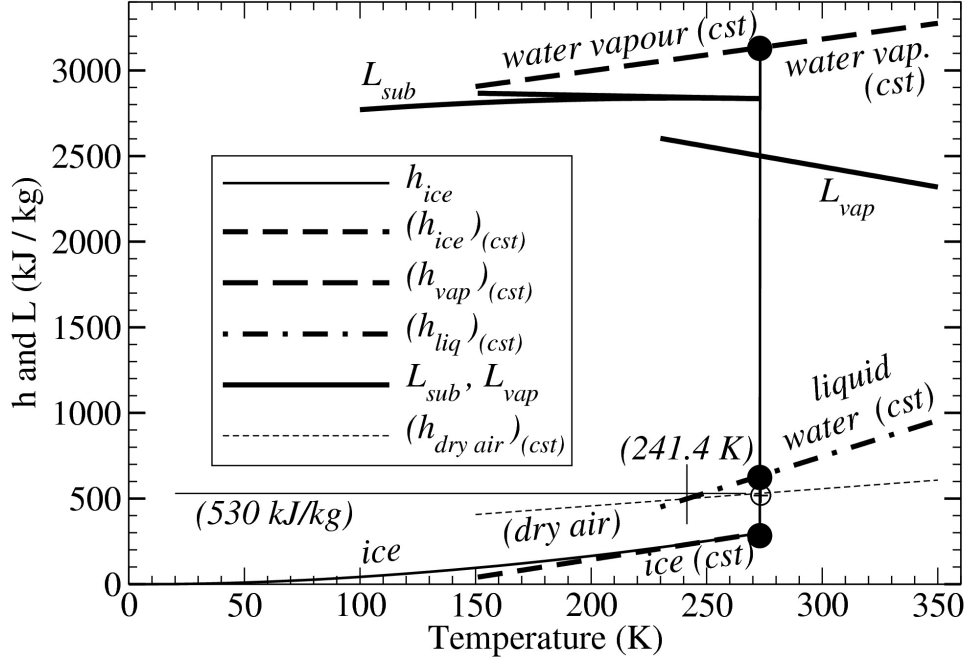


Figure 8: *Enthalpies for dry-air and water species as a function of the absolute temperature, with units of kJ kg^{-1} . The enthalpy of ice-Ih is plotted in the range of temperature from 0 to 273.15 K (thin solid line). The three dashed lines represent the ice, liquid-water and water-vapour enthalpies computed with “constant specific heat capacity” assumptions ($c_i = 2106$, $c_l = 4218$ and $c_{pv} = 1846.1 \text{ J K}^{-1} \text{ kg}^{-1}$). The three bold dots represent the standard values $h_i^0 \approx 298$, $h_l^0 \approx 632$ and $h_v^0 \approx 3133 \text{ J kg}^{-1}$. Latent heat curves are described in the text.*

could be small terms in comparison with the latent heat $L_{vap}(T_0)$. A large vertical step is indeed observed at T_0 in Figure 8 between the water vapour and both liquid-water and dry-air enthalpies. This means that L_{vap}^0 is the dominant term in this diagram.

The reason why the latent heat of vaporization for H_2O is much larger than those for N_2 or O_2 (2501 versus 200 and 213 kJ kg^{-1}) is due to Trouton’s rule (Wisniak, 2001). This rule states that almost all substances follow the general result $L_{vap}/T \approx 88 \text{ J mol}^{-1} \text{ K}^{-1}$ at their boiling temperature and at normal pressure of 1000 hPa. The dominant feature for L_{vap}^0 is thus a consequence of the boiling temperature of H_2O (373.15 K), which is about 4.4 times greater than those for N_2 (77.4 K) and O_2 (90 K).

The consequence of the coincidence $h_d^0 \approx h_l^0$ and of Trouton’s rule is that $c_{pd} T_\gamma \approx c_{pd} T_0 \Upsilon_0 \approx L_{vap}^0$ is valid to within 5 %. The last term of (40) can thus be approximated by $L_{vap} q_t$, leading to the approximate formula for the thermal enthalpy of moist air

$$h \approx h_{ref} + c_{pd} T + L_{vap} q_v - L_{fus} q_i. \quad (51)$$

Unlike (40), this approximate formula is not symmetric if $L_{vap} q_l$ is replaced by $L_{sub} q_i$, since it is the term $L_{fus} q_i$ that is involved in (51). This means that the internal liquid-ice symmetry of the enthalpy equation (40) may not be observed in approximate versions of h .

The results presented in this section show the extent to which the thermodynamic properties of water are special and different from the properties of dry air. The coincidence $h_d^0 \approx h_l^0$ and Trouton’s rule associated with the high boiling temperature of H_2O are empirical results. Since it is possible to avoid these approximations, and since they can lead to systematic errors, theoretical investigation dealing with moist-air thermal enthalpy should be based on the more general formula (40). Otherwise, some physical properties might be poorly represented or misinterpreted.

4.2 Analytic comparisons between enthalpy and two MSE quantities.

The structures of $h + \phi$, with h given by (40) or by the approximation (51), are clearly similar to the MSE quantities recalled in Section 2.7, except for the constant term h_{ref} , which has no physical meaning since it corresponds to a global shift in the moist enthalpy units. It will be shown in the following sections that $h + \phi$ is especially close to MSE_d and MSE_m given by (20) and (24).

Accordingly, in this section, comparisons are made between the analytical formulations of the thermal enthalpy $h - h_{ref}$ computed with (40) and the quantities TMSE_d and TMSE_m given by (20) and (24). The relative accuracies of the approximation of h by TMSE_d or TMSE_m are evaluated by the terms $X_d = [\text{TMSE}_d - (h - h_{ref})]/(c_{pd} T)$ and $X_m = [\text{TMSE}_m - (h - h_{ref})]/(c_{pd} T)$. After some algebra, they can be written as

$$X_d = \left(\frac{L_{vap}}{c_{pd} T} - \frac{T_\gamma}{T} - \lambda \right) q_t + \left(\frac{L_{fus}}{c_{pd} T} \right) q_i, \quad (52)$$

$$X_m = \left(\frac{L_{vap}}{c_{pd} T} - \frac{T_\gamma}{T} \right) q_t + \left(\frac{c_l - c_{pv}}{c_{pd}} \right) q_l + \left(\frac{c_i - c_{pv}}{c_{pd}} + \frac{L_{fus}}{c_{pd} T} \right) q_i. \quad (53)$$

Since the specific contents q_t , q_l and q_i are small terms (less than 0.03 kg kg^{-1}), X_h and X_h are less than 10 % if absolute values of the terms in parentheses in (52) and (53) are lower than 3.

The last two terms in parentheses in (53) can be approximated by 2.4 for q_l and 1.5 for q_i . The first term in parentheses in (53) can be evaluated from the results $T_\gamma \approx 2362 \text{ K}$ and $L_{vap}(T_0)/c_{pd} \approx 2490$, leading to a positive value of about 0.5 for the first quantity in factor q_t . Similarly, the first term in parentheses in (52) is about -0.4 at $T_0 = 273.15 \text{ K}$, and the second term in parentheses in (52) is equal to 1.7. If q_t is replaced by $q_v + q_l + q_i$, X_m and X_d can be approximated at T_0 by

$$X_m(T_0) \approx 0.5 q_v + 3 q_l + 2 q_i, \quad (54)$$

$$X_d(T_0) \approx -0.4 q_v - 0.4 q_l + 0.9 q_i. \quad (55)$$

X_m is thus a positive difference indicating that the larger the water species contents q_v and q_l are, the more TMSE_m overestimates the moist thermal enthalpy $h - h_{ref}$. Except for very high and unrealistic values of q_i , X_d is negative and TMSE_d underestimates $h - h_{ref}$. The specific ice content q_i further increases the overestimation of TMSE_m , while it decreases the underestimation of TMSE_d .

The approximations of $(h - h_{ref})$ by TMSE_m or TMSE_d can thus be considered as accurate for under-saturated conditions ($q_l = q_i = 0$), with X_m and $|X_d|$ lower than 1% for q_v lower than 20 g kg^{-1} . The differences become larger within clouds, and in particular for TMSE_m , with X_m increasing by about 0.3% for each 1 g kg^{-1} of liquid-water content.

Possible systematic differences of about 1% correspond to differences in T_h and T of about 3 K. This can be of some importance for the accurate determination of the moist thermal enthalpy within clouds or moist regions. Such large differences may modify the analysis of the impact of drying or moistening processes on h and on the local temperature. This is another justification for the use of the complete formula (40) when evaluating h , with no approximation for the second line depending on q_t .

4.3 Thermal enthalpy diagrams.

The possibility of computing specific moist values for the thermal enthalpy h offers the opportunity to plot the enthalpy diagram shown in Figure 9, where q_t is plotted as a function of h . This diagram is the enthalpy counterpart of the entropy diagram (q_t, s) given in Marquet and Geleyn (2013).

In this enthalpy diagram, the moist thermal enthalpy h given by (40) is compared with the quantity $h_{ref} + \text{TMSE}_m$, where $\text{TMSE}_m = c_p T + L_{vap} q_v$ is the thermal part of (24). The use of TMSE_m instead of h generates an error X_m measured by (53) and represented by the thin solid lines (values 0, 0.1, 0.5, 1, 3 and 5 %). Positive values of X_m correspond to dashed lines located to the right of the solid lines, or equivalently to $\text{TMSE}_m > h$. The water-vapour saturation pressure is computed with the liquid-water formulation if $T > 0$ C and with the ice formulation otherwise. This creates zigzag features for X_m in the saturated regions and around 0 C (about 535 kJ kg^{-1}).

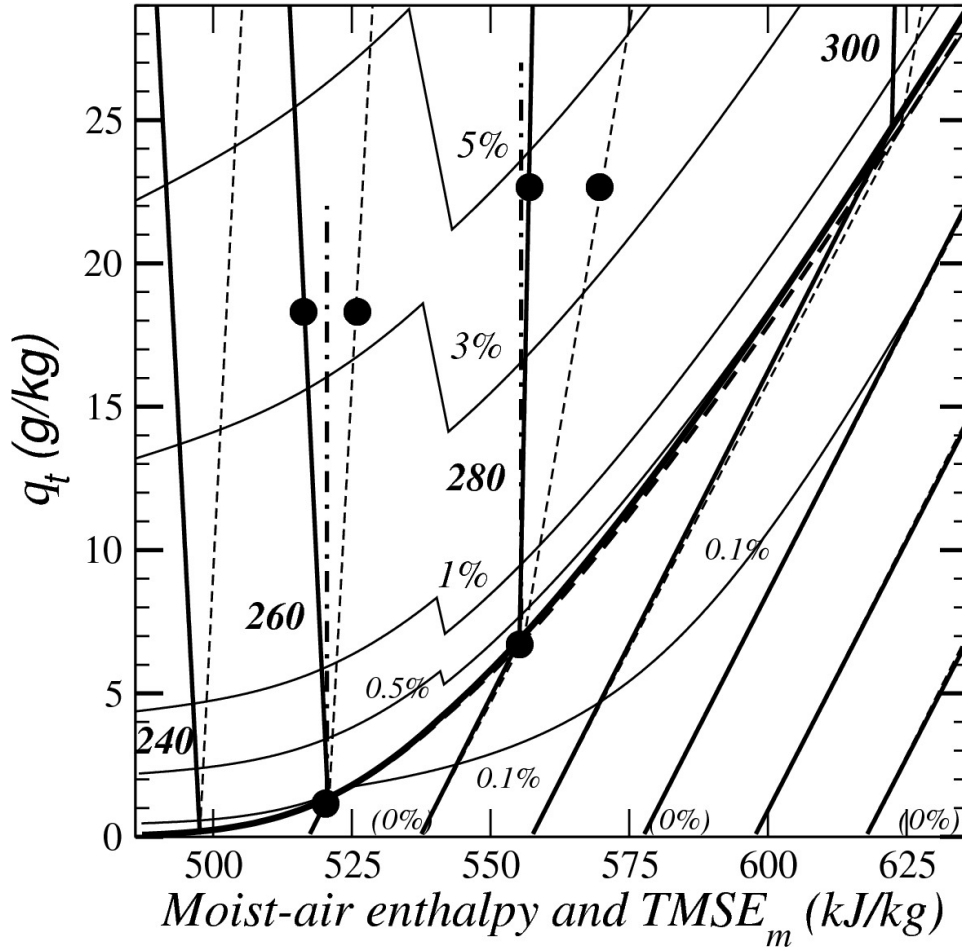


Figure 9: *Enthalpy diagram at the constant pressure $p_1 = 900 \text{ hPa}$. The total specific water content is plotted against the moist enthalpy h or against $h_{ref} + \text{TMSE}_m$, with $h_{ref} = h_d^0 = 530 \text{ kJ kg}^{-1}$. The saturation curves are plotted in the centre of the diagram (bold solid lines for h and dashed lines for TMSE_m). The saturated regions are located above the saturation curves. Isotherms are labelled every 20 K, with bold solid lines for h and dashed lines for TMSE_m . Other elements are described in the text.*

The isotherms are represented on Figure 9 for either h (solid lines) or $h_{ref} + \text{TMSE}_m$ (dashed lines) as abscissae (from 240 to 300 K by steps of 20 K). The two sets of isotherms are almost superimposed in the non-saturated domain. This means that the approximation $h \approx h_{ref} + \text{TMSE}_m$ is accurate in the non-saturated region, where X_m increases gradually from 0 % for the dry-air case to less than 0.1 % to 0.5 %, depending on the temperature. It is, however, worth noting that a value of 0.2% for X_m corresponds to large differences in T of about 0.6 K.

According to the formula (54), the approximations are greater in the saturated region (above the saturation curves), reaching 1 % for $q_l = 3 \text{ g kg}^{-1}$ or $q_i = 5 \text{ g kg}^{-1}$. Larger differences between moist thermal enthalpy and TMSE_m values are indeed observed in the saturated region of the enthalpy Figure 9.

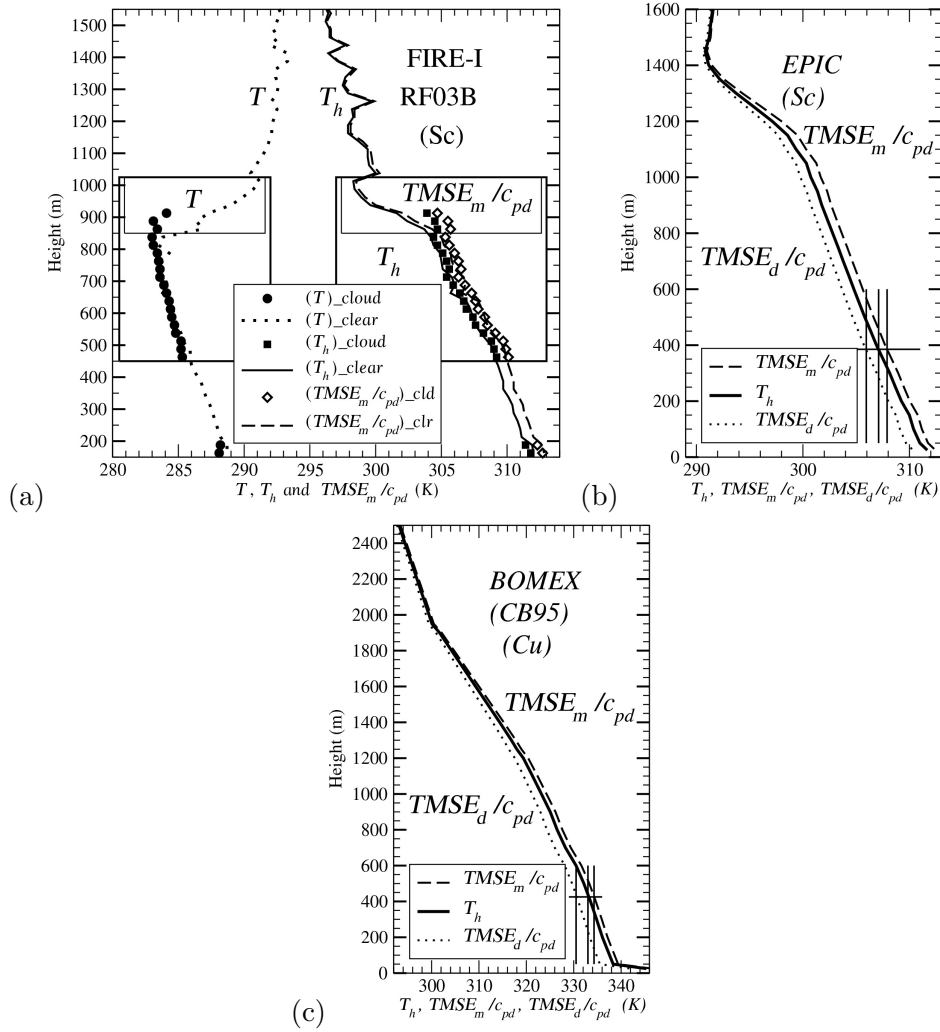


Figure 10: (a) The stratocumulus FIRE-I RF03B (2 July 1987) data flight. The temperature T is depicted as a dotted line for clear-air conditions and as dark circles for in-cloud regions. The enthalpy temperature T_h and $TMSE_m/c_{pd}$ are represented by a solid line and dark squares for T_h (clear-air and in-cloud regions) and by a bold dashed line and open diamonds for $TMSE_m/c_{pd}$ (clear-air and in-cloud regions). (b) The EPIC stratocumulus vertical profile and (c) the BOMEX shallow cumulus vertical profile, where the profiles of $TMSE_d/c_{pd}$ are plotted. Thin vertical solid lines highlight differences between T_h , $TMSE_m/c_{pd}$ and $TMSE_d/c_{pd}$.

The black spots represent moistening processes associated with large isothermal increases of q_t which originate at the saturation line at 260 and 280 K. These processes correspond to a decrease in h in the ice region and to almost constant values in the liquid-water domain. Conversely, $TMSE_m$ exhibits a clear increase with q_t in the saturated domains and for the whole range of temperatures.

Although increases of more than 15 g kg^{-1} for q_t are large and unrealistic, this is only for the sake of clarity and the same kind of changes in h or $TMSE_m$ are observed for smaller and more realistic increases of q_t . These differences suggest that $TMSE_m$ does not give an accurate measurement of the thermal enthalpy for saturated moist air, because they correspond to different physical properties. Such differences may be observed within stratocumulus or cumulus clouds, implying possible systematic biases for the impacts of entrainment and detrainment processes on the budget of moist enthalpy (and thus on the local temperature).

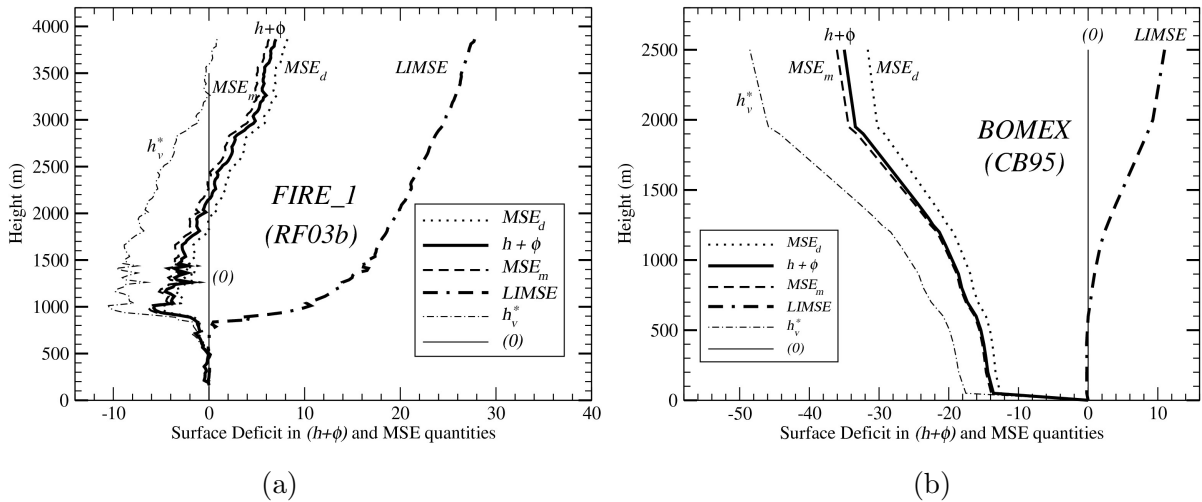


Figure 11: Vertical profiles of surface deficit of $h + \phi$ and of several MSE quantities defined in (20)-(24) for (a) the FIRE-I (RF03b) stratocumulus and (b) the BOMEX shallow cumulus. Units are in kJ kg^{-1} .

4.4 Evaluations of T_h and two TMSE quantities for stratocumulus and cumulus profiles.

Vertical profiles of T_h , $TMSE_m$ and $TMSE_d$ are compared in Figures 10(a)-(c) for two stratocumulus cases (FIRE-I and EPIC) and one shallow cumulus case (BOMEX). They correspond to the datasets given in Appendix C. Cloud liquid-water contents are small, but the values of q_v in the PBL are large enough to allow clear evaluations of impacts of water vapour. For the sake of readability, vertical profiles of $TMSE_d$ are not plotted for FIRE-I in (a).

A large positive top-of-PBL jump in T is associated with large negative jumps in both T_h and $TMSE_m/c_{pd}$ in (a). Moreover, in-cloud and clear-air values are different in the entrainment region represented by the thin solid line boxes. These results are different from the important properties observed in M11 with the same dataset but with moist entropy, where it is shown that in-cloud and clear-air values of θ_s are almost equal and almost constant in the whole PBL, including in the entrainment region at the top. It can be concluded that the specific moist enthalpy represented by T_h is not conserved (nor well-mixed) by the moist turbulence within the PBL of FIRE-I stratocumulus, contrary to what happens for the specific moist entropy.

The approximation of (54) suggests that $TMSE_m/c_{pd}$ is warmer than the enthalpy temperature T_h , due to the term $0.5 q_v$, whereas (55) suggests that $TMSE_d/c_{pd}$ is cooler, due to the term $-0.4 q_v$. This is observed for all profiles (a)-(c), where $TMSE_m$ overestimates T_h (and thus the moist enthalpy) by about 1 K in the warm and moist lower troposphere, whereas $TMSE_d$ underestimates T_h by about 2 K for EPIC and BOMEX.

According to (52) to (55), the three formulations for h , $TMSE$ and $TMSE_d$ are the same in the dry-air limit ($q_v = q_l = q_i = 0$). This is confirmed by the vertical profiles depicted on Figures 10(a)-(c): the curves converge above the top of the PBL, where q_v is small.

In order to investigate the comparison between enthalpy and MSE quantities differently, vertical profiles of deficit in surface values are shown in Figure 11(a) for the FIRE-I stratocumulus case and in (b) for the BOMEX shallow cumulus case. This kind of surface-deficit chart is commonly used in studies of convective processes.

It is shown that MSE_m , $h + \phi$ and MSE_d remain close to each other at each level and for the two cases, with the generalized enthalpy located between the others and with MSE_m being a better approximation for $h + \phi$. This confirms the results observed in Figures 10(a) and (c).

In Figure 11(a)-(b), $LIMSE$ and h_v^* are more different from $h + \phi$ than MSE_m and MSE_d . This

means that the thermal part of LIMSE and h_v^* cannot represent the moist-air thermal enthalpy h accurately.

Large jumps in all variables are observed close to the surface for BOMEX, except for LIMSE, due to the impact of large values of surface specific humidity that are not taken into account in LIMSE. The impact of surface values are not observed for FIRE-I, since the in-flight measurements were taken at altitude.

The conclusion of this section is that MSE_m is probably the best candidate for approximating $h + \phi$. However, the fact that systematic differences exist between h and MSE quantities in the moist lower PBL only, and not in the dry air above, may have significant physical implications if the purpose is to accurately analyse moist enthalpy budgets or differential budgets, or to understand the convective processes (entrainment and detrainment), or to validate the long-term budgets for NWP models and GCMs by comparing them with climatology or reanalyses.

4.5 Wet-bulb temperatures and psychrometric equations.

The differences between $h + \phi$ and MSE quantities observed in Figures 9 to 11 can be interpreted in a different way. If enthalpy is replaced in abscissa by temperature, the enthalpy of Figure 9 is transformed into the psychrometric chart plotted on Figure 12, where the isotherms are vertical.

The aim of psychrometric charts is to determine and plot the lines of constant wet-bulb temperature T_w . It is assumed in N21 or DVM75 that T_w is the temperature attained by a mass of moist air brought to saturation by water evaporating into it, with a latent heat continuously supplied by the wet bulb. It is thus an isenthalpic process at constant pressure for the whole system of the moist air plus the wet bulb, with the mass of dry air assumed to be constant. The WMO (2008) psychrometric equation is derived in DVM75. It can be written as

$$(c_{pd} + c_{pv} r_v) (T - T_w) = L_{vap}(T_w) (r_{sw} - r_v). \quad (56)$$

The wet-bulb temperature may be defined differently. The left hand side is approximated by $c_{pd} (T - T_w)$ in N21. The definition (6.67) or (6.78) published in Bohren and Albrecht (1998) corresponds to $c_{pv} r_v$ being replaced by $c_l r_{sw}$. Psychrometric equations are derived in E94 (4.6.4) and A10 (5.41) by assuming conservation of h_v^*/q_d expressed per unit mass of dry air. They correspond to $c_{pv} r_v$ being replaced by $c_{pv} r_l + (c_{pv} - c_l) r_v$. All these terms depending on mixing ratios are expected to be small in comparison with c_{pd} in (56).

The wet-bulb temperature may be derived from the Second Law and the conservation of the pseudo-adiabatic potential temperature θ'_w . It is the temperature attained by a parcel of fluid brought adiabatically to saturation by upward displacement and at a lower pressure, then carried adiabatically back to the original pressure, with water assumed to be continuously supplied to maintain saturation.

Psychrometric lines of equal T_w and lines of constant θ'_w are plotted on Figure 12. The figure shows that the versions of N21 and DVM75 are very close to each other. This is a confirmation that $c_{pd} (T - T_w)$ is the leading-order term in (56). Larger differences are observed with lines of constant θ'_w , in particular for $RH < 50$ %. The wet-bulb temperatures computed from the methods described in N21 or DVM75 and the one using θ'_w are thus different.

It is common practice to plot isenthalpic lines on the same psychrometric charts. These lines of constant specific enthalpy expressed per unit mass of dry or moist air correspond to open systems, since values of $q_t = q_v$ vary from 0 to the saturating value q_{sw} . We thus have an opportunity to compare the properties of h given by (40) with those from MSE formulations, because MSE quantities are derived for closed systems only and with arbitrary assumptions like $h_d^0 = h_l^0$ at 0° C, whereas the definition of h is valid for both closed and open systems *a priori* and is derived from a Third Law. This study is the continuation of the comparison of h and $TMSE_m$ in the Figure 9.

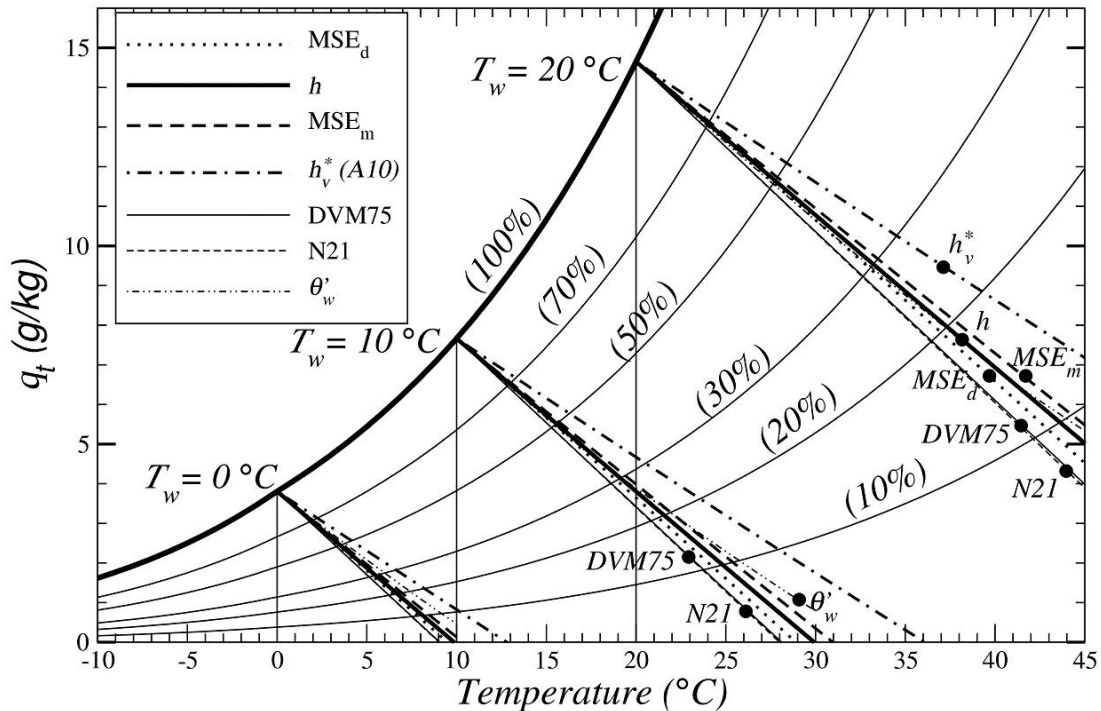


Figure 12: Psychrometric diagram for 1000 hPa and for $\phi = 0$. Vertical isotherms and lines of constant T_w (thin solid lines) are for $T_w = 0^{\circ}\text{C}$, 10°C and 20°C in a non-saturation region (where $q_l = q_i = 0$). The two versions derived from DVM75 and N21 can be compared using lines of constant θ'_w . Bold lines for constant enthalpy (h) or MSE quantities (MSE_d , MSE_m and h_v^*) decrease with T . Lines of constant relative humidity curve upwards (from 70% to 10%), the saturation curve corresponding to 100%.

All isenthalpic lines are oriented in a downward direction on Figure 12. They are almost parallel to psychrometric lines of constant values of T_w , but do not coincide with them. This probably invalidates the possibility that psychrometric lines might be computed as constant values of h , although additional measurements are required to determine which curve is relevant for low RH.

Moreover, systematic differences exist on Figure 12: the curves of constant h are located between the curves of constant MSE_d and MSE_m , whereas the curves of constant h_v^* are more different and are located above the others. The closed system assumption and the use of arbitrary definitions for the reference enthalpies explain the differences observed between the curves plotted with h and with other MSE quantities.

5 Discussion and conclusion.

In the same way that moist entropy is expressed in M11 in terms of $c_{pd} \ln(\theta_s)$ up to a constant entropy reference value, moist-air thermal enthalpy is expressed in terms of $c_{pd} T_h$ up to a constant enthalpy reference value. The potential temperature θ_s and the enthalpy temperature T_h are thus equivalent to the specific moist-air entropy (s) and thermal enthalpy (h).

Thermal enthalpies are generated by variations of $c_p(T)$ with T corresponding to progressive excitations of the translational, rotational and vibrational states of the molecules, and by possible changes of phase represented by latent heats (with negligible impact of changes of pressure).

The original feature is that both T_h and θ_s depend on standard values of enthalpies and entropies, via the terms Υ_r and Λ_r , respectively. In this paper, standard values are determined with an error of a few percent for the cryogenic properties of the dry-air and water-components of moist air. Different choices for these standard values would generate other values for T_h and

θ_s . The use of cryogenic values for the specific heats of solid and liquid phases, in addition to latent heats when changes of phases occur, eliminate the issue of referring to the perfect gas law when the temperature is too low.

The important feature in the definition of h and s is that the specific contents of the moist-air components multiply several constant terms which depend on the reference values T_r or p_r . This leads naturally to additional varying terms depending on q_t . It is for this reason that the standard values h_d^0 , h_v^0 , s_d^0 and s_v^0 must be determined for varying q_t . This explains why the Third Law versions for h and s are different from the ones obtained in DVM75, E94 or P10, where only quantities per unit of dry-air are considered and where hypotheses like $h_d^0 = 0$, $h_l^0 = 0$, $h_v^0 = 0$ or $h_d^0 = h_l^0$ are made at a temperature different from 0 K. This suggests that the Third Law of thermodynamics may have an important and somewhat surprising physical meaning when moist-air thermodynamics is considered.

The constant volume or constant dry-air point of view may be useful for laboratory experiments, but it is not relevant to isolate the dry-air part from a moving open moist-air parcel with multiple components. The specific value approach is more suitable for applications to a barycentric view and to equations of compressible fluids. This may explain some of the differences between the present Third Law results and previous ones.

It has been shown that the enthalpy temperature is expressed in terms of the quantity T_Υ , which depends on the difference between the standard values of dry-air and water-vapour enthalpies (in the same way as the moist entropy depends, via Λ_r , on the difference between the standard values of dry-air and of water-vapour entropies).

It should be noted that T_Υ is a constant term independent of the reference temperature T_r . This means that the same property observed by entropy in M11 is also valid for the thermal enthalpy, i.e. they are both independent of the choice made for the reference temperature and pressure T_r and p_r . Since they are well-defined local quantities, it becomes possible to use specific values of thermal enthalpy or entropy to compute local budgets, integral or mean values of h and s , either in space or time.

A more surprising result concerns the assumption that generalized enthalpy might be roughly represented by MSE_m or MSE_d . It is shown that it is serendipitous since: i) the numerical values of standard enthalpies of dry air and liquid water are close to each other; and ii) L_{vap}^0 is a large dominant term of T_Υ .

It is shown in M11 that no such coincidence exists for the entropy, thus explaining the large impact of the new term Λ_r introduced for the entropy computations. However, even if MSE_m or MSE_d might be considered as relevant approximations of $h + \phi$ (at least for non-saturated conditions), they do not follow the same internal liquid-ice symmetry as in the case of the specific moist-air enthalpy formulation.

The enthalpy diagram illustrates the possibility of representing all the thermodynamic properties of moist air as a function of h , p and q_t alone, as in Pauluis and Schumacher (2010) who suggest using the set (s, p, q_t) to compute any of the basic variables (T, p, q_v, q_l, q_i) . It is thus possible to use the First- or Second-Law set of variables (h, p, q_t) or (s, p, q_t) as prognostic variables. This is true for LES models where each grid cell represents a homogeneous parcel of moist air (as long as the pressure is known, in spite of non-hydrostatic processes).

This result is no longer valid for a parcel subject to sub-grid variability. All properties of a parcel in NWP models or GCMs are understood as weighted sums of properties observed for a given fraction of unsaturated air plus the other part from saturated air (with weighting factors depending on cloud fractions). However, the method of representing moist-air properties by (s, p, q_t) or by (h, p, q_t) may be used even in NWP models or GCMs, provided that: it is i) applied separately for each of the unsaturated and saturated fractions of moist air, and ii) the values of cloud fraction can be determined by some other processes.

It thus becomes possible to compute and study the tendencies of h or s generated by various processes (dynamics, radiation, convection, turbulence) and to compare the results with reanalysis outputs. An alternative method could consist of evaluating the finite differences $h(t + dt) - h(t)$ at each point, or $s(t + dt) - s(t)$, with the specific thermal enthalpy or entropy computed with zero values at 0 K.

Another application concerns pure isenthalpic processes, as plotted on psychrometric charts. It is shown in this paper that, depending on how the specific enthalpy is defined, the isenthalpic lines are different. Since there is only one kind of isenthalpic process in the real world, it might be valuable to compare the new thermal enthalpy versions involving real processes and/or observations.

The differences between MSE quantities and $h + \phi$ are analysed for several cumulus and stratocumulus vertical profiles. MSE_m is greater, and MSE_d smaller, than the generalized enthalpy $h + \phi$ in moist conditions. These systematic differences of more than 1% may have significant physical implications for the accurate determination of the moist thermal enthalpy within clouds. They may modify results from analyses of the impact of drying or moistening processes on h , and therefore on local temperature. This confirms the striking results obtained when referring to the enthalpy diagrams, and suggests that the formulation of thermal enthalpy (40) should be used to compute moist enthalpy or energy budgets accurately. This may be important for the validation of NWP models and/or GCMs, when the budget of thermal enthalpy simulated by these models is compared with those obtained from climatology or reanalyses.

All of the above suggests new possible applications for the Third Law formulation of entropy and thermal enthalpy. It may be used to study dry-air entrainment and moist-air detrainment occurring along cloud edges, as well as the conservative properties used when parameterizing shallow or deep-convection. For the latter phenomena, MSE quantities should be replaced by the specific generalized enthalpy $h + \phi$.

Acknowledgements

The author is most grateful to Jean-François Geleyn and Maarten Ambaum for stimulating discussions. He would like to thank the anonymous referees for their constructive comments, which helped to improve the manuscript. Thanks to S. Becker and Y. Tourre for the improvements of the written English. S. R. de Roode and Q. Wang kindly provided the validation data from NASA Flights during the FIRE I experiment.

Appendix A. List of symbols and acronyms.

c_{pd}	specific heat of dry air	(1004.7 J K ⁻¹ kg ⁻¹)
c_{pv}	spec. heat of water vapour	(1846.1 J K ⁻¹ kg ⁻¹)
c_l	spec. heat of liquid water	(4218 J K ⁻¹ kg ⁻¹)
c_i	spec. heat of ice	(2106 J K ⁻¹ kg ⁻¹)
c_p	specific heat at constant pressure for moist air	($c_p = q_d c_{pd} + q_v c_{pv} + q_l c_l + q_i c_i$)
δ	$= R_v/R_d - 1 \approx 0.608$	
η	$= 1 + \delta = R_v/R_d \approx 1.608$	
ε	$= 1/\eta = R_d/R_v \approx 0.622$	
κ	$= R_d/c_{pd} \approx 0.2857$	
γ	$= \eta \kappa = R_v/c_{pd} \approx 0.46$	
λ	$= c_{pv}/c_{pd} - 1 \approx 0.8375$	
e	water-vapour partial pressure	
$e_{sw}(T)$	partial saturating pressure over liquid water	
e_r	water-vapour reference partial pressure:	$e_r = e_{ws}(T_r = T_0) \approx 6.11$ hPa
e_i	internal energy:	$e_i = h - p/\rho = h - R T$

g	magnitude of Earth's gravity: $9.8065 \text{ m}^2 \text{ s}^{-2}$
h	specific enthalpy
$(h_d)_r$	reference enthalpy of dry air at T_r
$(h_v)_r$	reference enthalpy of water vapour at T_r
h_d^0	standard specific enthalpy of dry air at T_0 (530 kJ kg ⁻¹)
h_v^0	standard specific enthalpy of water vapour at T_0 (3133 kJ kg ⁻¹)
h_l^0	standard specific enthalpy of liquid water at T_0 (632 kJ kg ⁻¹)
h_i^0	standard specific enthalpy of ice water at T_0 (298 kJ kg ⁻¹)
h_v^*	a specific moist static energy (A10)
Λ_r	$= [(s_v)_r - (s_d)_r]/c_{pd} \approx 5.87$
L_{vap}	$= h_v - h_l$: latent heat of vaporization
L_{vap}^0	$= 2.501 \cdot 10^6 \text{ J kg}^{-1}$ at T_0
L_{fus}	$= h_l - h_i$: latent heat of fusion
L_{fus}^0	$= 0.334 \cdot 10^6 \text{ J kg}^{-1}$ at T_0
L_{sub}	$= h_v - h_i$: latent heat of sublimation
L_{sub}^0	$= 2.835 \cdot 10^6 \text{ J kg}^{-1}$ at T_0
m	a mass of moist air
p	$= p_d + e$: local value of pressure
p_r	$= (p_d)_r + e_r$: reference pressure ($p_r = p_0$)
p_d	local dry-air partial pressure
$(p_d)_r$	reference dry-air partial pressure ($\equiv p_r - e_r$)
p_0	$= 1000 \text{ hPa}$: conventional pressure
q_d	$= \rho_d/\rho$: specific dry air content
q_v	$= \rho_v/\rho$: specific water vapour content
q_l	$= \rho_l/\rho$: specific liquid water content
q_i	$= \rho_i/\rho$: specific ice content content
q_t	$= q_v + q_l + q_i$: total specific water content
q_s	specific for saturating water vapour content
r_v	$= q_v/q_d$: mixing ratio for water vapour
r_l	$= q_l/q_d$: mixing ratio for liquid water
r_i	$= q_i/q_d$: mixing ratio for ice
r_r	reference mixing ratio for water species: $\eta r_r \equiv e_r/(p_d)_r$ and $r_r \approx 3.82 \text{ g kg}^{-1}$
r_s	mixing ratio for saturating water vapour
r_t	$= q_t/q_d$: mixing ratio for total water
ρ_d	specific mass of dry air
ρ_v	specific mass of water vapour
ρ_l	specific mass of liquid water
ρ_i	specific mass of ice
ρ	specific mass of moist air ($\rho = \rho_d + \rho_v + \rho_l + \rho_i$)
RH	relative humidity ($100 \times e/e_{sw}$ for liquid water)
R_d	dry-air gas constant (287.06 J K ⁻¹ kg ⁻¹)
R_v	water-vapour gas constant (461.53 J K ⁻¹ kg ⁻¹)
R	$= q_d R_d + q_v R_v$: gas constant for moist air
s	specific entropy
$(s_d)_r$	reference values for the entropy of dry air,
$(s_v)_r$	reference values for the entropy of water vapour,
s_d^0	standard specific entropy of dry air at T_0 and p_0 : 6775 J K ⁻¹ kg ⁻¹
s_v^0	standard specific entropy of water vapour at T_0 and p_0 : 10320 J K ⁻¹ kg ⁻¹
s_l^0	standard specific entropy of liquid water at T_0 and p_0 : 3517 J K ⁻¹ kg ⁻¹
s_i^0	standard specific entropy of solid water at T_0 and p_0 : 2296 J K ⁻¹ kg ⁻¹
S_e, S_l	entropies in P10 (S_a is their weighted sum)
T	local temperature

T_r	reference temperature ($T_r \equiv T_0$)
T_w	isenthalpic wet-bulb temperature
T_{il}	ice-liquid water temperature
T_0	zero Celsius temperature (273.15 K)
T_Υ	a constant temperature (2362 K)
θ	$= T (p_0/p)^\kappa$: potential temperature
θ_e	equivalent potential temperature
θ_l	liquid-water potential temperature
θ'_w	pseudo-adiabatic wet-bulb potential temperature
θ_s	moist entropy potential temperature (M11)
Υ_r	$= [(h_v)_r - (h_d)_r]/(c_{pd} T_r)$, $\Upsilon_0(T_0) \approx 9.5$
v_k, v	individual and barycentric mean velocities
J_k	individual barycentric diffusion flux
w	vertical component of the velocity
∇	3D-gradient operator
μ	Gibbs' function ($h - T s$)
b_k	$= (h_k)_r - c_{pk} T_r$ for species k (B82)
d_e, d_i	external and internal changes
\dot{Q}	diabatic heating rate
\dot{q}_v, \dot{q}_l	rate of change of q_v and q_l
\dot{S}_{irr}	irreversible source of entropy
ϕ	gravitational potential energy ($= g z + \phi_0$)
GCM	General Circulation Model
NWP	Numerical Weather Prediction
MSE	Moist Static Energy
LES	Large Eddy Simulation
TMSE	Thermal Moist Static Energy

Appendix B. Standard values of enthalpies.

The values of the specific heat of oxygen are given in Table B.1 for the 0 to 300 K range of temperature. The resulting variation of $c_p(T)$ is depicted in Figure 4.

According to Fagerstroem and Hollis Hallet (1969, hereafter referred to as FH69), the solid α - β transition occurs at about 23.85 K, with no latent heat associated with it. The solid β - γ transition occurs at about 43.78 K with a latent heat of 23.2 kJ kg⁻¹. The latent heat of melting occurring at the triple point (54.4 K) is equal to 13.9 kJ kg⁻¹. The latent heat of vaporization occurring at 90 K is equal to 213 kJ kg⁻¹.

The specific heat for the liquid phase of O₂ is about 2 J K⁻¹ mol⁻¹ lower in Jacobsen *et al.* (1997), giving an indication on the level of accuracy (≈ 4 %) in the measurements of properties of cryogenic substances.

The values of the specific heat of nitrogen are given in Table B.2 for the 0 to 300 K range of temperature. The resulting variation of $c_p(T)$ is depicted in Figure 5.

According to Manzhelii and Freiman (1997, hereafter referred to as MF97), the solid α - β transition occurs at about 35.6 K and the associated latent heat is equal to 8.2 kJ kg⁻¹. This latent heat is equal to 7.7 kJ kg⁻¹ in Lipiński *et al.* (2007), with a discrepancy in the values illustrating the errors (≈ 6 %) made in measurements of properties of cryogenic substances. The latent heat of melting at the triple point (63.1 K) is equal to 25.7 kJ kg⁻¹ in MF97. The latent heat of vaporization at 77.4 K is equal to 200 kJ kg⁻¹.

The values of the specific heat of ice-Ih are given in Table B.3 for the range of temperatures from 0 to 273 K. The resulting variation of $c_p(T)$ is depicted in Figure 6.

Table B.1: Values of the specific heat for O₂ are given as a function of the absolute temperature. The first table corresponds to the solid- α form. Units are K for T and J K⁻¹ mol⁻¹ for c_p , to be divided by 0.032 kg mol⁻¹ to obtain units of J K⁻¹ kg⁻¹. Data were obtained up to 20 K from Table-I of FH69, with some interpolation performed from their Figures 1 and 2 for the range 21 to 23.84 K. The second table corresponds to the solid- β form. Data were obtained from Table I of FH69 for the range 30 to 43.78 K, with interpolation performed from their Figures 1 and 2 for the range 23.855 to 28 K. The third table corresponds to the solid- γ form (43.78 to 54.4 K) and the fourth table to the liquid form (54.4 to 90 K). Data were obtained from FH69, with linear interpolation from their Figure 1. The fifth table corresponds to the vapour form at 1013.25 hPa (above 90 K) and with c_p directly expressed in J K⁻¹ kg⁻¹. Data were obtained from Jacobsen *et al.* (1997, Table 5.79).

$c_p(T)$ for O₂ (solid- α) - Unit of J K⁻¹ mol⁻¹

T	c_p	T	c_p	T	c_p
0	0	12	4	23	23
2	0.01	13	5	23.35	30
3	0.05	14	6	23.52	40
4	0.12	15	7.1	23.6	50
5	0.24	16	8.3	23.68	70
6	0.43	17	9.6	23.71	100
7	0.72	18	11.1	23.76	200
8	1.12	19	12.5	23.80	500
9	1.65	20	14	23.82	1000
10	2.30	21	16	23.84	2000
11	3.10	22	18.2		

$c_p(T)$ for O₂ (solid- β) - Unit of J K⁻¹ mol⁻¹

T	c_p	T	c_p	T	c_p
23.855	2000	24.03	50	28	26
23.860	1000	24.10	40	30	28
23.865	500	24.32	30	35	34
23.87	200	25	23.2	40	41
23.88	100	26	23.7	43.78	45.4
23.91	70	27	24.7		

$c_p(T)$ for O₂ (solid- γ) - Unit of J K⁻¹ mol⁻¹

T	c_p	T	c_p	T	c_p
43.78	45.4	50	46	54.4	46.5

$c_p(T)$ for O₂ (liquid) - Unit of J K⁻¹ mol⁻¹

T	c_p	T	c_p	T	c_p
54.4	55	70	55.66	90	56.5

$c_p(T)$ for O₂ (vapour) - Unit of J K⁻¹ kg⁻¹

T	c_p	T	c_p	T	c_p
90	970.5	135	923.1	240	914.5
95	941.3	140	921.8	250	915.0
100	935.2	145	920.7	260	915.6
105	933.2	150	919.6	270	916.4
110	931.6	170	916.7	280	917.4
115	929.8	190	915.1	290	918.5
120	928.0	210	914.3	300	919.9
125	926.2	230	914.3		
130	924.6	235	914.4		

Table B.2: Values of the specific heat for N_2 are given as a function of the absolute temperature. The first table corresponds to the solid- α form. Data were obtained up to 35.6 K from Table-14.4 of MF97. Units are K for T and $J K^{-1} mol^{-1}$ for c_p , to be divided by $0.028016 kg mol^{-1}$ to obtain units of $J K^{-1} kg^{-1}$. The second table corresponds to the solid- β form. Data were obtained up to 56 K directly from Table-14.4 of MF97. The data in the range 56 to 63 K were obtained from the measured values depicted on Figure 1 of Kudryavtsev and Nemchenko (2001), with a change in the slope of the curve $c_p(T)$. The third and fourth tables correspond to the liquid and the vapour forms (at 1013.25 hPa) and with c_p directly expressed in $J K^{-1} kg^{-1}$. Data were obtained from Jacobsen *et al.* (1997, Table 5.73).

T	c_p	T	c_p	T	c_p
0	0	20	19.9	30	31.16
2	0.03	21	21.37	31	35.80
4	0.24	22	22.86	32	37.64
6	0.91	23	24.24	33	39.77
8	2.43	24	25.67	33.5	40.97
10	4.83	25	27.05	34	42.16
12	7.64	26	28.45	34.5	43.38
14	10.66	27	29.82	35	44.63
16	13.61	28	31.19	35.3	45.53
18	16.64	29	32.64	35.6	45.91

$c_p(T)$ for N_2 (solid- α) - Unit of $J K^{-1} mol^{-1}$

T	c_p	T	c_p	T	c_p
35.6	36.08	44	39.27	56	43.5
36	36.26	46	40.03	58	44.5
38	37.02	48	40.78	60	45.5
39	37.39	50	41.53	62	46.5
40	37.76	52	42.29	63.1	47.0
42	38.52	54	43.04		

$c_p(T)$ for N_2 (solid- β) - Unit of $J K^{-1} mol^{-1}$

T	c_p	T	c_p	T	c_p
63.1	2019	70	2015	77.4	2042

$c_p(T)$ for N_2 (liquid) - Unit of $J K^{-1} kg^{-1}$

T	c_p	T	c_p	T	c_p
77.4	1340	120	1056	200	1043
80	1191	140	1050	250	1042
90	1081	160	1047	300	1041
100	1067	180	1045		

$c_p(T)$ for N_2 (vapour) - Unit of $J K^{-1} kg^{-1}$

Table B.3: Values of the specific heat for the solid (ice-Ih) form of H₂O as a function of the absolute temperature. Data were obtained up to 273 K from Table-13 of Feistel and Wagner (2006) and at a pressure of 1013.25 hPa. Units are K for T and J K⁻¹ kg⁻¹ for c_p .

$c_p(T)$ for H₂O (ice-Ih) - Unit of J K⁻¹ kg⁻¹

T	c_p	T	c_p	T	c_p
0	0	100	874.14	200	1568.35
10	14.80	110	949.38	210	1638.86
20	111.43	120	1021.30	220	1710.03
30	230.66	130	1090.80	230	1781.79
40	337.89	140	1158.82	240	1854.08
50	437.49	150	1226.18	250	1926.83
60	532.56	160	1293.51	260	1999.98
70	623.92	170	1361.21	270	2073.48
80	711.48	180	1429.53	273	2095.59
90	794.93	190	1498.57		

As for O₂ and N₂, the thermal enthalpy of the water species are obtained from (41) by integrating the values of $c_p(T)$ shown in Figure 6 and by summing all the corresponding latent heats, which leads to a standard thermal enthalpy for ice at T_0 of $h_l(T_0) \approx 298$ kJ kg⁻¹. The latent heat of fusion and sublimation at temperature T_0 are 334 kJ kg⁻¹ and 2835 kJ kg⁻¹, respectively, leading to the standard values $h_l(T_0) \approx 632$ kJ kg⁻¹ and $h_v(T_0) \approx 3133$ kJ kg⁻¹.

From (50) the standard value of thermal enthalpy for ice (298 kJ kg⁻¹) is in good agreement with the value suggested in Feistel and Wagner (2006), Table 14, from which $h_i(T_0) - h_i(0) \approx 298.35$ kJ kg⁻¹.

Conversely, Bannon, 2005 (hereafter referred to as B05) used the Thermochemical Tables of Chase, 1998 (hereafter referred to as C98) to evaluate dry-air and water-vapour enthalpies as 273.5 and 503.1 kJ kg⁻¹, respectively. The large differences with the corresponding results derived in this section (530 and 3133 kJ kg⁻¹) can be explained by the choice of different definitions of the (thermal) enthalpy in C98, where only the integral of the vapour value of c_p from 0 to T are computed. The contribution of the latent heats (solid-solid, solid-liquid and liquid-vapour), or the integral of the liquid or solid values of c_p at low temperature (including Debye's law) are not taken into account in C98.

For the water vapour, if the latent heat of sublimation (2835 kJ kg⁻¹) is roughly added to the value 503.1 kJ kg⁻¹ deduced from C98, the result 3338 is close to, but greater than, the value of $h_v^0 = 3133$ kJ kg⁻¹ given in (44). But the integral of the ice values of c_p , with c_p varying from 0 to 2106 J K⁻¹ kg⁻¹ as shown in Figure 6, must be smaller than if the integral is computed with the almost constant water-vapour value 1846.1 J K⁻¹ kg⁻¹. This must explain why the value 3338 used in C98 and B05 is greater than the value of 3133 computed in this Appendix: it corresponds to the integral of almost constant vapour (perfect gas?) values of c_p .

The sum of the latent heats described in Figures 4 and 5 are equal to 250 for O₂ and 234 kJ kg⁻¹ and N₂. If the corresponding dry-air average value 237 is added to the value 273.5 found in B05, the result 511 kJ kg⁻¹ is close to, but smaller than, the value $h_d^0 = 530$ kJ kg⁻¹ given in (43). This difference can be explained by the integral of the solid and liquid values of c_p which are greater than the vapour values extrapolated toward 0 K, as shown in Figures 4 and 5.

Appendix C. Stratocumulus and Cumulus datasets.

Numerical values used for plotting the Figures 10 (a)-(c) and 11 (a)-(b) are described in this Appendix.

Table B.4: The dataset for FIRE-I (in-cloud).

Z (m)	p (hPa)	T (K)	q_v (g/kg)	q_l (g/kg)
912.5	915.5	284.13	7.58	0.089
887.5	917.5	283.13	8.21	0.163
862.5	920.1	283.37	8.20	0.140
837.5	922.9	283.01	8.20	0.153
812.5	926.0	283.15	8.27	0.132
787.5	928.8	283.39	8.36	0.094
762.5	931.7	283.48	8.41	0.078
737.5	933.7	283.63	8.46	0.066
712.5	936.9	283.64	8.38	0.054
687.5	939.7	283.86	8.48	0.050
662.5	942.2	284.08	8.57	0.044
637.5	944.6	284.26	8.62	0.034
612.5	947.3	284.37	8.66	0.030
587.5	950.0	284.49	8.80	0.028
562.5	952.8	284.66	8.84	0.019
537.5	955.3	284.84	8.97	0.023
512.5	958.7	285.20	9.07	0.017
487.5	961.2	285.20	9.13	0.044
462.5	962.7	285.30	9.18	0.037

The same FIRE-I (RF03B) dataset as used in M11 is given in Tables B.4 and B.5 for in-cloud and clear-air values, respectively. Values are defined every 25 m up to 3862.5 m in the Figures. Only a few selected levels are kept above 1562.5 m in Table B.5. Liquid water contents reach a maximum (0.163 g kg^{-1}) close to 900m.

The EPIC dataset is given in Table B.6. It corresponds to the LES profiles of (θ, q_v, q_l) given in Bretherton *et al.* (2004) for a 6-day mean sounding in October 2001. Liquid water contents reach a maximum of 0.283 g kg^{-1} at 1200m.

The BOMEX dataset is given in Table B.7. It corresponds to the LES profiles depicted in Cuijpers and Bechtold (1995) for (θ_l, q_t) . Liquid water content is less than 0.01 g kg^{-1} for this shallow cumulus (Siebesma *et al.*, 2003) and is set to 0 for this application.

Table B.5: The dataset for FIRE-I (clear-air).

Z (m)	p (hPa)	T (K)	q_v (g/kg)	Z (m)	p (hPa)	T (K)	q_v (g/kg)
3862.5	645.7	280.37	1.03	987.5	906.5	290.66	2.97
3562.5	668.7	282.08	1.04	962.5	909.4	289.88	3.44
3062.5	710.3	285.41	1.27	937.5	912.4	289.01	4.08
2562.5	753.8	287.86	1.17	912.5	914.9	287.32	5.48
2062.5	799.7	290.38	1.12	887.5	917.6	286.39	6.17
1562.5	847.7	292.55	1.36	862.5	920.3	286.83	6.49
1537.5	850.3	292.81	1.39	837.5	923.4	283.76	7.87
1512.5	852.4	292.51	1.42	787.5	929.9	284.25	7.96
1487.5	855.1	292.23	1.63	762.5	931.3	283.83	8.13
1462.5	858.0	292.64	1.47	612.5	947.6	284.64	8.68
1437.5	860.8	292.04	2.17	587.5	950.1	284.75	8.72
1412.5	862.8	293.32	1.19	562.5	953.0	284.91	8.72
1387.5	864.5	293.34	1.43	537.5	956.0	285.20	8.78
1362.5	867.6	292.38	2.27	512.5	958.7	285.28	8.94
1337.5	870.1	292.40	2.05	487.5	962.1	285.86	8.88
1312.5	872.8	292.57	1.88	462.5	963.3	285.85	8.91
1287.5	875.4	292.49	2.08	437.5	966.7	285.96	8.96
1262.5	878.2	292.08	2.92	412.5	969.2	286.35	8.89
1237.5	880.4	292.45	2.20	387.5	972.6	286.66	8.84
1212.5	883.1	292.35	2.27	362.5	975.4	286.90	8.75
1187.5	885.8	292.09	2.22	337.5	978.4	287.13	8.82
1162.5	888.3	292.06	2.25	312.5	981.3	287.39	8.85
1137.5	891.0	291.89	2.63	287.5	984.1	287.58	8.80
1112.5	893.7	291.69	2.94	262.5	986.9	287.80	8.82
1087.5	896.4	291.34	3.10	237.5	989.8	288.03	8.81
1062.5	899.0	290.94	3.31	212.5	992.7	288.20	8.81
1037.5	901.9	290.53	3.64	187.5	996.3	288.72	8.90
1012.5	904.3	291.20	2.73	162.5	997.3	288.67	8.97

Table B.6: The dataset for EPIC.

Z (m)	p (hPa)	T (K)	q_v (g/kg)	q_l (g/kg)
1600	827.6	288.66	1.10	0.0
1550	832.5	288.48	1.10	0.004
1500	837.4	288.21	1.15	0.033
1450	842.4	287.70	1.20	0.075
1400	847.4	286.71	1.70	0.175
1350	852.4	285.66	2.50	0.200
1300	857.5	283.95	3.75	0.262
1250	862.5	282.41	5.00	0.267
1200	867.7	281.50	6.00	0.283
1150	872.8	280.87	6.80	0.250
1100	878.0	280.62	7.20	0.204
1050	883.2	280.57	7.60	0.150
1000	888.4	280.60	7.75	0.104
950	893.7	280.84	7.90	0.067
900	899.0	281.12	7.95	0.031
850	904.3	281.50	8.00	0.008
800	909.7	281.88	8.05	0.003
750	915.1	282.25	8.10	0.001
700	920.5	282.68	8.12	0.0
650	926.0	283.11	8.15	0.0
600	931.5	283.54	8.17	0.0
550	937.0	283.97	8.20	0.0
500	942.6	284.40	8.23	0.0
450	948.2	284.86	8.27	0.0
400	953.8	285.32	8.30	0.0
350	959.4	285.80	8.35	0.0
300	965.1	286.28	8.40	0.0
250	970.9	286.77	8.42	0.0
200	976.6	287.25	8.45	0.0
150	982.4	287.74	8.55	0.0
100	988.2	288.13	8.55	0.0
50	994.1	288.71	8.50	0.0
25	997.0	289.00	8.70	0.0
0	1000.0	288.80	9.10	0.0

Table B.7: The dataset for BOMEX.

Z (m)	p (hPa)	T (K)	q_v (g/kg)
2500	751.4	285.32	3.00
2400	760.0	285.96	3.24
2300	768.8	286.60	3.48
2200	777.6	287.24	3.72
2100	786.6	287.88	3.96
2000	795.6	288.52	4.20
1950	800.2	288.62	4.40
1900	804.7	288.67	5.00
1800	814.0	288.76	5.94
1700	823.4	288.86	6.88
1600	832.8	288.95	7.82
1500	842.4	289.04	8.76
1400	852.1	289.12	9.70
1300	861.9	289.25	10.60
1250	866.8	289.34	11.00
1200	871.8	289.43	11.50
1100	881.8	289.80	12.10
1000	892.0	290.36	12.60
900	902.2	290.92	13.10
800	912.6	291.58	13.40
700	923.1	292.29	13.80
600	933.7	292.95	14.40
500	944.4	293.81	14.70
400	955.3	294.67	14.90
300	966.3	295.69	15.00
200	977.4	296.66	15.10
100	988.6	297.63	15.30
50	994.3	298.11	15.40
25	997.1	298.46	17.95
0	1000.0	298.80	20.50

References

- Betts AK. 1973 (B73). Non-precipitating cumulus convection and its parameterization. *Q. J. R. Meteorol. Soc.* **99** (419): 178–196.
- Ambaum MHP. 2010. Thermal physics of the atmosphere. Advancing weather and climate science. Wiley-Blackwell. John Wiley and sons. Chichester (A10).
- Arakawa A, Schubert WH. 1974. Interaction of a cumulus cloud ensemble with the large-scale environment, Part I. *J. Atmos. Sci.* **31** (3): 674–701 (AS73).
- Bannon PR. 2005. Eulerian available energetics in moist atmosphere. *J. Atmos. Sci.* **62** (12): 4238–4252 (B05).
- Bechtold P, Bazile E, Guichard F, Mascart P, Richard E. 2001. A mass-flux convection scheme for regional and global models. *Q. J. R. Meteorol. Soc.* **127** (573): 869–886.
- Betts AK. 1973. Non-precipitating cumulus convection and its parameterization. *Q. J. R. Meteorol. Soc.* **99** (419): 178–196 (B73).
- Betts AK. 1974. Further comments on “A comparison of the equivalent potential temperature and the static energy”. *J. Atmos. Sci.* **31** (6): 1713–1715 (B74).
- Betts AK. 1975. Parametric interpretation of Trade-Wind cumulus budget studies. *J. Atmos. Sci.* **32** (10): 1934–1945 (B75).
- Bretherton CS, Uttal T, Fairall CW, Yuter SE, Weller RA, Baumgardner D, Comstock K, Wood R, Raga GB. 2004. The EPIC 2001 Stratocumulus study. *Bull. Amer. Meteor. Soc.* **85**, (7): 967–977.
- Bretherton CS, Blossey PN., Khairoutdinov M. 2005. An energy-balance analysis of deep convective self-aggregation above uniform SST. *J. Atmos. Sci.* **62** (12): 4273–4292.
- Bohren CF, Albrecht BA. 1998. Atmospheric thermodynamics. Pp.1–402. Oxford University Press.
- Bougeault Ph. 1985. A simple parameterization of the large-scale effects of cumulus convection. *Mon. Wea. Rev.* **113** (12): 2108–2121.
- Businger JA. 1982. The fluxes of specific enthalpy, sensible heat and latent heat near the Earth’s surface. *J. Atmos. Sci.* **39** (8): 1889–1892 (B82).
- Catry B, Geleyn JF, Tudor M, Bénard P, Trojáková A. 2007. Flux-conservative thermodynamic equations in a mass-weighted framework. *Tellus A.* **59**, (1): 71–79.
- Chase MW Jr. 1998. Journal of Physics and Chemical Reference Data. Monograph No.9. NIST-JANAF Thermochemical Tables. 4th ed. *American Chemical Society and American Institute of Physics.* Vol.1, Pp. 1–957. Vol.2, Pp. 959–1951 (C98).
- Cuijpers JWM, Bechtold P. 1995. A simple parameterization of cloud water related variables for use in boundary layer models. *J. Atmos. Sci.* **52** (13): 2486–2490.
- De Groot SR, Mazur P. 1962. Non-equilibrium Thermodynamics. *North-Holland Publishing Company.* Amsterdam
- Derbyshire SH, Beau I, Bechtold P, Grandpeix J-Y, Piriou J-M, Redelsperger J-L, Soares PMM. 2004. Sensitivity of moist convection to environmental humidity. *Q. J. R. Meteorol. Soc.* **130** (604): 178–196.
- Dufour L, Van Mieghem J. 1975. Thermodynamique de l’atmosphère. Institut Royal Météorologique de Belgique. Bruxelles (DVM75).
- Emanuel KA. 1994. Atmospheric convection. Pp.1–580. Oxford University Press: New York and Oxford (E94).
- Emanuel KA. 2004. Tropical cycle energetics and structure. Chapter 8 in “Atmospheric

- Turbulence and mesoscale meteorology. Scientific Research Inspired by Doug Lilly.” Edited by E.E. Fedorovich, R. Rotunno and B. Stevens. p:165-192. Cambridge University Press.
- Fagerstroem CH., Hollis Hallet AC. 1969. The specific heat of solid oxygen. *Journal of low temperature Physics.* **1** (1). 3–12 (FH69).
 - Feistel R., Wagner W. 2006. A new equation of state for H₂O ice Ih. *J. Phys. Chem. Ref. Data* **35** (2). 1021–1047.
 - Fuehrer PL, Friche CA. 2002. Flux corrections revisited. *Boundary-Layer Meteorol.* **102** (3): 415-457.
 - Gerard L, Piriou J-F, Brozkova R, Geleyn J-F, Banciu D. 2009. Cloud and precipitation parameterization in a meso-gamma-scale operational weather prediction model. *Mon. Wea. Rev.* **137** (11): 3960–3977.
 - Glansdorff P, Prigogine I. 1971. Structure stabilité et fluctuations. *Masson Ed.* Paris (Also available in English: Thermodynamic theory of structure, stability and fluctuations, Wiley-Interscience).
 - Iribarne JV., Godson WL. 1973. Atmospheric thermodynamics. *Geophysics and astrophysics monographs. D. Reidel Pub. Company.* Dordrecht-Holland and Boston-U.S.A.
 - Hauf T, Höller H. 1987. Entropy and potential temperature. *J. Atmos. Sci.* **44** (20): 2887–2901 (HH87).
 - Jacobsen RT, Penoncello SG, Lemmon EW. 1997. Thermodynamic properties of Cryogenic fluids. Pp.1–312. The international cryogenics monograph series. Springer, New-York.
 - Khairoutdinov MF, Randall DA. 2003. Cloud resolving modeling of the ARM summer 1997 IOP: model formulation, results, uncertainties, and sensitivities. *J. Atmos. Sci.* **60** (4): 607–625.
 - Kudryavtsev IN, Nemchenko KE. 2001. Lattice dynamics and heat capacity of solid nitrogen. Proceeding of the 10th international conference on phonon scattering in condensed matter. August 12-17, 2001. Dartmouth, USA.
 - Lipiński L, Kowal A, Szmyrka-Grzebyk A, Manuszkiewicz H, Steur PPM., Pavese F. 2007. The α - β transition of Nitrogen. *Int. J. Thermophys.* **28**. 1904–1912.
 - Madden RA, Robitaille FE. 1970. A comparison of the equivalent potential temperature and the static energy. *J. Atmos. Sci.* **27** (2): 327–329.
 - Manzhelii VG, Freiman YA. 1997. Physics of Cryocrystals. Pp.1–691. Springer, New-York.
 - Marquet P. 1993. Exergy in meteorology: definition and properties of moist available enthalpy. *Q. J. R. Meteorol. Soc.* **119** (511): 567–590.
 - Marquet P. 2011. Definition of a moist entropic potential temperature. Application to FIRE-I data flights. *Q. J. R. Meteorol. Soc.* **137** (656): 768–791 (M11). <http://arxiv.org/abs/1401.1097>. arXiv:1401.1097 [ao-ph]
 - Marquet P, Geleyn J-F. 2013. On a general definition of the squared Brunt-Väisälä frequency associated with the specific moist entropy potential temperature. *Q. J. R. Meteorol. Soc.* **139** (670) : 85–100. <http://arxiv.org/abs/1401.2379>. arXiv:1401.2379 [ao-ph]
 - Marquet P. 2013. On the definition of a moist-air potential vorticity. *Q. J. R. Meteorol. Soc.* Accepted in April, 2013. Early view stage <http://arxiv.org/abs/1401.2006>. arXiv:1401.2006 [ao-ph]
 - Nagle JF. 1966. Lattice statistics of Hydrogen bonded crystals. I. The residual entropy of Ice. *J. Math. Phys.* **7** (8): 1484–1491.
 - Normand CWB. 1921. Wet bulb temperatures and the thermodynamics of the air. *Indian Metl. Memoirs.* **23**. Part 1: 1–22 (N21).

- Pauling L. 1935. The structure and entropy of ice and of other crystals with some randomness of atomic arrangement. *J. Am. Chem. Soc.* **57** (12): 2680–2684.
- Pauluis O., Czaja A, Korty R. 2010. The global atmospheric circulation in moist isentropic coordinates. *J. Climate.* **23**. 3077–3093 (P10).
- Pauluis O., Schumacher J. 2010. Idealized moist Rayleigh-Bénard convection with piecewise linear equation of state. *Commun. math. Sci.* **8** (1): 295–319.
- Peterson TC., Willett KM., Thorne PW. 2011. Observed changes in surface atmospheric energy over land. *Geophys. Res. Lett.* **38** (L16707): 1–6.
- Richardson LF. 1922. Weather prediction by numerical process. *Cambridge University Press* (R22).
- Saunders PM. 1957. The thermodynamics of saturated air: a contribution to the classical theory. *Q. J. R. Meteorol. Soc.* **83** (357): 342–350.
- Siebesma AP, Bretherton CS, Brown A, Chlond A, Cuxart J, Duynkerke PG, Jiang H, Khairoutdinov M, Lewellen D, Moeng CH, Sánchez E, Stevens B, Stevens DE. 2003. A large eddy simulation intercomparison study of shallow cumulus convection. *J. Atmos. Sci.* **60** (10): 1870–1891.
- Tripoli GJ, Cotton WR. 1981. The use of ice-liquid water potential temperature as a thermodynamic variable in deep atmospheric models. *Mon. Weather Rev.* **109**, (5) : 1094–1102.
- Wisniak J. 2001. Frederick Thomas Trouton: the man, the rule, and the ratio. *Chem. Educator.* **6** (1): 55–61.
- WMO-No.8. 2008. Guide to meteorological instruments and methods of observation. 7th edition. *World Meteorological Organization.*
- Zdunkowski W, Bott A. 2004. Thermodynamics of the atmosphere. A course in theoretical meteorology. *Cambridge University Press.*